

**DOES INSPIRATORY RESISTIVE LOADING CAUSE EXPIRATORY MUSCLE
FATIGUE?**

by

Carli Monica Peters

B.Sc. (hons), Mount Allison University, 2012

A THESIS SUBMITTED IN PARTIAL FULFILLMENT OF
THE REQUIREMENTS FOR THE DEGREE OF

MASTER OF SCIENCE

in

THE FACULTY OF GRADUATE AND POSTDOCTORAL STUDIES

(Kinesiology)

THE UNIVERSITY OF BRITISH COLUMBIA

(Vancouver)

December 2015

© Carli Monica Peters, 2015

Abstract

Expiratory resistive loading (ERL) elicits inspiratory as well as expiratory muscle fatigue, suggesting parallel co-activation of the inspiratory muscles during expiration. It is unknown whether the expiratory muscles are similarly co-activated to the point of fatigue during inspiratory resistive loading (IRL). The purpose of this study was to determine whether IRL elicits expiratory as well as inspiratory muscle fatigue. Male subjects (n=10) underwent isocapnic IRL to task failure (60% maximal inspiratory pressure, 15 breaths/min, 0.7 inspiratory duty cycle). Abdominal and diaphragm contractile function was assessed at baseline and at 3, 15 and 30 min post-IRL by measuring gastric twitch pressure ($P_{ga,tw}$) and transdiaphragmatic twitch pressure ($P_{di,tw}$) in response to potentiated magnetic stimulation of the thoracic and phrenic nerves, respectively. Electromyographic activity of the diaphragm, rectus abdominis, and external oblique was monitored to ensure consistency of stimulation. Fatigue was defined as >15% reduction from baseline in $P_{ga,tw}$ or $P_{di,tw}$. During IRL (mean \pm SE; 11.9 ± 2.5 min), mean arterial pressure and heart rate increased in a time-dependent manner (13 mmHg and 50 beats/min for the final min, respectively). $P_{di,tw}$ was significantly lower than baseline (34.1 ± 3.2 cmH₂O) at 3 min (23.2 ± 1.9 cmH₂O, $p < 0.05$) and 15 min post-IRL (24.2 ± 1.7 cmH₂O, $p < 0.05$). $P_{ga,tw}$ was not significantly different from baseline after IRL. These results suggest that IRL elicits objective evidence of diaphragm, but not abdominal, muscle fatigue. Agonist-antagonist interactions for the respiratory muscles appear to be more important during ERL than during IRL. Future studies attempting to characterize the physiological consequences of diaphragm fatigue, without the confounding effects of abdominal fatigue, can use IRL to induce diaphragm fatigue.

Preface

This thesis contains original data collected and analyzed for partial fulfilment of Carli Peters' Master of Science degree. All protocols were approved by the University of British Columbia's Clinical Research Ethics Board (approval number: H14-01208). The research question and experimental protocol were developed by Carli Peters and Drs William Sheel, Lee Romer, and Don McKenzie. Data was collected and analyzed by Carli Peters.

Table of Contents

Abstract.....	ii
Preface.....	iii
Table of Contents	iv
List of Tables	vii
List of Figures.....	viii
List of Abbreviations	x
Acknowledgements	xii
Dedication	xiii
Introduction.....	1
Hypothesis.....	5
Methods.....	6
Subjects	6
Experimental Overview	6
Measurements and Procedures.....	7
Pulmonary function.....	7
Respiratory pressures	7
Magnetic stimulation of the diaphragm	8
Magnetic stimulation of the abdominals.....	8
Electromyography	8
Consistent stimulation.....	9
Contractile function and membrane excitability.....	9
Reproducibility of twitch pressures	10

Inspiratory resistive loading.....	10
Data collection and processing	11
Data Analysis	11
Consistent stimulation.....	11
Contractile function and membrane excitability.....	11
Respiratory and cardiovascular variables during IRL	12
Statistical analysis.....	12
Results	13
Descriptive data	13
Consistent stimulation.....	14
Inspiratory resistive loading.....	20
Fatigue.....	24
Reproducibility of twitch measures	33
Subject 1.....	33
Subject 5.....	36
Subject 9.....	40
Discussion	45
Major finding	45
Fatigue.....	45
Abdominal fatigue	46
Diaphragm fatigue	47
Mechanisms of diaphragm fatigue.....	49
Eliciting the respiratory muscle metaboreflex	50

End-tidal CO ₂ during IRL.....	51
Reproducibility of twitch measures	52
Methodological considerations	54
Conclusions.....	56
References.....	57
Appendix A: Individual subject data	62

List of Tables

Table 1: Descriptive characteristics of all subjects.....	13
Table 2: Physiological responses during rest, the first 6 min, and final min of loading.....	21
Table 3: Subject 1 between-day gastric twitch ramp reproducibility	34
Table 4: Subject 1 within-day reproducibility of baseline gastric twitch	35
Table 5: Subject 1 between-day reproducibility of baseline gastric twitch	35
Table 6: Subject 5 between-day gastric twitch ramp reproducibility	37
Table 7: Subject 5 between-day reproducibility of baseline gastric twitch	38
Table 8: Subject 5 between-day transdiaphragmatic twitch ramp reproducibility	39
Table 9: Subject 5 between-day reproducibility of baseline transdiaphragmatic twitch	40
Table 10: Subject 9 between-day gastric twitch ramp reproducibility	41
Table 11: Subject 9 between-day reproducibility of baseline gastric twitch	42
Table 12: Subject 9 between-day transdiaphragmatic twitch ramp reproducibility	43
Table 13: Subject 9 between-day reproducibility of baseline transdiaphragmatic twitch	44
Table 14: Individual descriptive data for all subjects.	62

List of Figures

Figure 1: Group mean transdiaphragmatic twitch pressure and gastric twitch pressure in response to 1-Hz magnetic stimulation of increasing stimulation intensity.	15
Figure 2: Left and right diaphragm M-wave area in response to 1-Hz magnetic stimulation of increasing stimulation intensity.	16
Figure 3: Left and right diaphragm M-wave amplitude in response to 1-Hz magnetic stimulation of increasing stimulation intensity.	17
Figure 4: Rectus abdominis and external oblique M-wave area in response to 1-Hz magnetic stimulation of increasing stimulation intensity.	18
Figure 5: Rectus abdominis and external oblique M-wave amplitude in response to 1-Hz magnetic stimulation of increasing stimulation intensity.	19
Figure 6: Raw data from a representative subject during rest, first min, second min, and final min of inspiratory loading protocol.	22
Figure 7: Heart rate and mean arterial pressure at rest, during the first 6 min, and final min of inspiratory loading protocol.	23
Figure 8: Example of individual transdiaphragmatic and gastric twitch pressure responses to 1-Hz magnetic stimulation at baseline, 3 min post-, 15 min post-, and 30 min post-IRL from a representative subject.	25
Figure 9: Group mean transdiaphragmatic and gastric twitch pressure in response to 1-Hz magnetic stimulation at baseline, 3 min post-, 15 min post-, and 30 min post-IRL.	26
Figure 10: Group mean % change from baseline for transdiaphragmatic and gastric twitch pressure in response to 1-Hz magnetic stimulation at baseline, 3 min post-, 15 min post-, and 30 min post-IRL.	27
Figure 11: Left and right diaphragm M-wave area in response to 1-Hz magnetic stimulation at baseline, 3 min post-, 15 min post-, and 30 min post-IRL.	28
Figure 12: Left and right diaphragm M-wave amplitude in response to 1-Hz magnetic stimulation at baseline, 3 min post-, 15 min post-, and 30 min post-IRL.	29
Figure 13: Rectus abdominis and external oblique M-wave area in response to 1-Hz magnetic stimulation at baseline, 3 min post-, 15 min post-, and 30 min post-IRL.	30
Figure 14: Rectus abdominis and external oblique M-wave amplitude in response to 1-Hz magnetic stimulation at baseline, 3 min post-, 15 min post-, and 30 min post-IRL.	31

Figure 15: Relationship between cumulative force output and fatigue of the diaphragm and abdominals for all subjects.....	32
Figure 16: Individual transdiaphragmatic and gastric twitch pressures in response to 1-Hz magnetic stimulation of increasing stimulation intensity	63
Figure 17: Individual left and right diaphragm M-wave areas in response to 1-Hz magnetic stimulation of increasing stimulation intensity	64
Figure 18: Individual left and right diaphragm M-wave amplitudes in response to 1-Hz magnetic stimulation of increasing stimulation intensity	65
Figure 19: Individual rectus abdominis and external oblique M-wave areas in response to 1-Hz magnetic stimulation of increasing stimulation intensity	66
Figure 20: Individual rectus abdominis and external oblique M-wave amplitudes in response to 1-Hz magnetic stimulation of increasing stimulation intensity.....	67
Figure 21: Individual heart rate and blood pressure data at rest, during the first 6 min, and during the final min of inspiratory loading.	68
Figure 22: Individual transdiaphragmatic and gastric pressure percent changes from baseline at 3 min-, 15 min-, and 30 min-post IRL.....	69
Figure 23: Individual left and right diaphragm M-wave area in response to 1-Hz magnetic stimulation at baseline, 3 min post-, 15 min post-, and 30 min post-IRL.....	70
Figure 24: Individual left and right diaphragm M-wave amplitude in response to 1-Hz magnetic stimulation at baseline, 3 min post-, 15 min post-, and 30 min post-IRL.....	71
Figure 25: Individual rectus abdominis and external oblique M-wave area in response to 1-Hz magnetic stimulation at baseline, 3 min post-, 15 min post-, and 30 min post-IRL.	72
Figure 26: Individual rectus abdominis and external oblique M-wave amplitude in response to 1-Hz magnetic stimulation at baseline, 3 min post-, 15 min post-, and 30 min post-IRL.	73

List of Abbreviations

Abbreviation	Definition
ANOVA	Analysis of variance
AP	Arterial blood pressure
CO ₂	Carbon dioxide
DBP	Diastolic blood pressure
EELV	End-expiratory lung volume
EMG	Electromyographic
EO	External oblique
ERL	Expiratory resistive loading
F _b	Breathing frequency
FEV ₁	Forced expiratory volume in 1 second
FRC	Functional residual capacity
FVC	Forced vital capacity
HR	Heart rate
IRL	Inspiratory resistive loading
MAP	Mean arterial pressure
MEP	Maximal expiratory pressure
MIP	Maximal inspiratory pressure
MSNA	Muscle sympathetic nerve activity
pCO ₂	Partial pressure of carbon dioxide
$\int p_{di}/dt$	Integral of transdiaphragmatic pressure over time

P_{di}	Transdiaphragmatic pressure
P_{diMAX}	Maximal transdiaphragmatic pressure
$P_{di,tw}$	Transdiaphragmatic twitch pressure
P_{es}	Esophageal pressure
$P_{es,tw}$	Esophageal twitch pressure
P_{ETCO_2}	Partial pressure of end-tidal carbon dioxide
$\int P_{ga}/dt$	Integral of gastric pressure over time
P_{ga}	Gastric pressure
P_{gaMAX}	Maximal gastric pressure
$P_{ga,tw}$	Gastric twitch pressure
P_m	Mouth pressure
RA	Rectus abdominis
SBP	Systolic blood pressure
SD	Standard deviation
SE	Standard error of the mean
T_I/T_{TOT}	Inspiratory duty cycle
TTI_{di}	Tension-time index of the diaphragm
\dot{V}_E	Minute ventilation
V_T	Tidal volume

Acknowledgements

I would like to acknowledge my supervisor, Dr. William Sheel, for his invaluable assistance over the past two years. I am excited to have the opportunity to continue to work with you over the next few years. I would also like to acknowledge my committee, Dr. Don McKenzie and Dr. Lee Romer, for their guidance throughout this study. By assisting me with developing my hypothesis, questioning how the experimental protocol I selected would test the hypothesis, and helping me troubleshoot data collection issues along the way, Drs Sheel, Romer, and McKenzie provided instrumental feedback on all aspects of my project. HIP lab members, thank you for all of your help with my experimental setup and data collection. Mom and Dad, thank you for supporting my decision to move across Canada and pursue a career in Academia. You both work very hard to give me the confidence to do whatever I set my mind to and I appreciate that more than you can possibly imagine. I would also like to thank Jen for listening to me vent on bad days, excitedly ramble on good days, and making this experience incredibly fun. Finally, thank you to my research subjects for donating their time.

Dedication

To Robbie P and T.

Introduction

The respiratory system is responsible for maintaining alveolar ventilation in proportion to metabolic demand, and the respiratory muscles play an integral role in meeting this challenge. The respiratory muscles can be broadly grouped into those that are active during inspiration and those that are active during expiration. The primary muscle of inspiration, the diaphragm, is a thin dome-shaped muscle that separates the abdominal and thoracic cavities. Accessory inspiratory muscles include the external intercostals, scalenes, and sternocleidomastoids. The primary expiratory muscles are the abdominal muscles, including the rectus abdominis, internal and external oblique muscles, and the transverse abdominis. Pressure gradients developed by the coordinated contraction of inspiratory and expiratory muscles facilitate airflow to and from the alveolar surface. Despite the crucial role they serve, which requires them to contract throughout their entire lifespan, the respiratory muscles, like other skeletal muscles, can fatigue in response to high ventilatory work ^{1,2}.

Skeletal muscle fatigue is defined as a reduction in force generating capacity or velocity-generating capacity after exposure to load that is reversible with rest ³. There are several steps between the motor cortex and the contractile machinery within the sarcomere that lead to force generation, and fatigue can occur at any step. The major potential sites of fatigue have been identified as: (1) excitatory input to higher motor centers; (2) excitatory drive to lower motor neurons; (3) motor neuron excitability; (4) neuromuscular transmission; (5) sarcolemma excitability; (6) excitation-contraction coupling; (7) contractile mechanisms; and (8) metabolic energy supply and metabolite accumulation ⁴. Processes in the spinal cord and above (steps 1-4)

are defined as central fatigue, whereas processes at or distal to the neuromuscular junction (steps 5-8) are defined as peripheral fatigue ⁴.

In the respiratory system, force generation capacity is usually estimated as pressure generation capacity, and several tests can be utilized to evaluate respiratory muscle pressure generation. Volitional pressure generation tests include maximal static inspiratory and expiratory pressure, sniff tests, and cough tests ⁵. Each of these tests has the advantage of being easy to perform and non-invasive. The disadvantage of volitional tests is that it is hard to determine whether a subject is making a truly maximal effort. Therefore, any reduction in pressures observed after an intervention of interest could be the result of central fatigue, peripheral fatigue, or a reduction in subject motivation or compliance. A more accurate assessment of respiratory muscle fatigue can be acquired with the use of non-volitional tests of muscle function. Fatigue is evident during non-volitional tests when there is a reduction in pressure generation relative to baseline in response to electrical or magnetic stimulation of the motor nerves that innervate the inspiratory or expiratory muscles. Utilization of nerve stimulation techniques removes the influence of the central nervous system and allows an objective assessment of peripheral fatigue. Commonly a balloon catheter system is used for assessing respiratory pressures during these tests. With this system, esophageal pressure (P_{es}) is measured as a surrogate for pleural pressure and gastric pressure (P_{ga}) as a reflection of abdominal pressure ⁶. Transducers attached to the proximal end of the catheters are used to monitor pressure throughout respiratory muscle function tests. The pressure difference across the diaphragm, referred to as transdiaphragmatic pressure (P_{di}), is obtained by measuring the pressure difference between P_{ga} and P_{es} . Expiratory abdominal muscle pressure generation is determined by measuring P_{ga} . P_{di} induced by

stimulation of the phrenic nerves ^{7,8} and P_{ga} induced by thoracic nerve root stimulation ⁹ provide non-volitional measures of the inspiratory diaphragm pressure and the expiratory abdominal pressure generation, respectively. It is well established that expiratory ² and inspiratory ¹ muscle peripheral fatigue occurs in response to high-intensity exercise and resistive loading ^{10,11}.

There are several physiological consequences of fatiguing contractions of inspiratory and expiratory muscles. Firstly, heightened perceptions of dyspnea occur in response to both inspiratory ¹² and expiratory muscle fatigue ^{13,14}. Secondly, inspiratory ¹⁵ and expiratory muscle fatigue ¹⁶ reduces subsequent exercise performance. Finally, high-intensity contractions of the inspiratory and expiratory muscles against resistive loads to the point of fatigue elicit a respiratory muscle metaboreflex ^{17,18}. The respiratory muscles, similar to limb skeletal muscles, are innervated by group III and IV afferent nerve fibers ^{19,20}. Contraction-induced stimuli activate molecular receptors of the group III and group IV nerve fibers, and this activation increases the spontaneous discharge of these muscle afferents ²¹. Inspiratory muscle fatigue induced by IRL in healthy humans causes an increase in muscle sympathetic nerve activity (MSNA) in the resting leg ¹⁷, a decrease in leg blood flow, and an increase in leg vascular resistance ¹¹. Mean arterial pressure (MAP) and heart rate (HR) also increase during fatiguing diaphragm contractions ¹¹. When the expiratory muscles are fatigued via ERL, a similar increase in MSNA is seen in the resting limb and an increase in MAP is observed ¹⁸. The physiological consequences of inspiratory and expiratory muscle fatigue are incredibly similar and therefore, the ability to determine the impact of each relies on our ability to isolate fatigue to just the inspiratory muscles or just the expiratory muscles. Often, inspiratory and expiratory loading

techniques are utilized to isolate fatigue to the inspiratory^{12,15} and expiratory muscles^{22,23}, respectively.

The effect of expiratory loaded breathing on inspiratory muscle fatigue has been previously investigated with inconsistent results. In some studies, maximum inspiratory pressure (MIP) was significantly reduced after exposure to an expiratory resistive load^{16,24}. However, in other studies expiratory loading had no effect on MIP^{22,23}. Indirect measures of respiratory muscle fatigue were used in all of these studies. More recently, magnetic stimulation was used to objectively assess inspiratory and expiratory muscle fatigue after ERL to task failure¹⁰. Subjects completed 4 different ERL trials on 4 different days. Breathing frequency was maintained at 15 breaths/min for all conditions, while expiratory duty cycle was maintained at 0.4 or 0.7 and expiratory P_{ga} at 40% or 60% of maximum (ERL_{40%0.4}, ERL_{70%0.4}, ERL_{40%0.7}, ERL_{70%0.7}). Transdiaphragmatic twitch pressure ($P_{di,tw}$) and gastric twitch pressure ($P_{ga,tw}$) were reduced below baseline values by 9-15% and 15-22%, respectively, after each ERL trial²⁵. Fatigue of the inspiratory muscles after ERL suggests co-activation of the inspiratory muscles when the load on the expiratory muscles is increased. The effects of ERL on inspiratory muscle fatigue may also apply to the expiratory muscles during inspiratory loading.

Previous work investigating the activity of abdominal muscles during inspiratory loading suggests that the abdominals are recruited when the load on the inspiratory muscles is increased^{26,27}. Recruitment of the abdominal muscles assists the inspiratory muscles in multiple ways. First, by reducing end expiratory lung volume (EELV), increases in tidal volume (V_T) can occur on the linear portion of the respiratory system compliance curve^{28,29}. Second, as EELV is

reduced, the diaphragm is lengthened. Lengthening of the diaphragm allows it to function at a more optimal length for tension development, according to the length-tension relationship of the muscle³⁰. Third, contraction of the abdominal muscles allows storage of elastic energy in the abdominal and thoracic walls that can be used to make up a portion of the energy required for the subsequent inspiration^{31,32}.

Currently, it is unknown whether the expiratory muscles are sufficiently co-activated during IRL to cause expiratory muscle fatigue. If fatigue of the expiratory muscles does occur in response to IRL, this will have implications for studies investigating the effect of inspiratory muscle fatigue on dyspnea, exercise tolerance, and MSNA. Therefore, the objective of this study is to determine whether IRL to task failure induces expiratory muscle fatigue.

Hypothesis

It is hypothesized that IRL to the point of task failure will induce fatigue of the expiratory muscles.

Methods

Subjects

Fourteen young (23-28 years), healthy men were recruited for testing. One subject withdrew before balloon catheters were placed. In another subject, balloon catheters moved during testing and a reliable assessment of twitch pressures could not be obtained. In two subjects there was a failure to stimulate the phrenic nerve and a reliable $P_{di,tw}$ could not be obtained. Data was analyzed from ten male subjects.

Experimental Overview

Upon arrival to the Health and Integrative Physiology Laboratory, subjects completed consent forms, followed by spirometry and anthropometric measures. All protocols were approved by the Clinical Research Ethics Board (approval number: H14-01208) at the University of British Columbia, which conforms to the *Declaration of Helsinki*. Surface electrodes were placed on the left and right side of subjects' diaphragm, and on the rectus abdominis (RA) and external oblique (EO) muscles. Balloon catheters were then passed pernasally into the stomach and esophagus. Measures of MIP and MEP were made once the balloons were in place. A magnetic stimulator was used to create recruitment curves for the diaphragm and the abdominal muscles by stimulating the phrenic and thoracic nerves, respectively. A pre-IRL assessment of contractile function and membrane excitability of the diaphragm and abdominal muscles was then performed. Subjects were then moved into the supine position where resting cardiovascular, respiratory and end-tidal CO₂ ($P_{ET}CO_2$) data were collected for a minimum of 5 min. Subjects remained in the supine position and performed an iso-capnic IRL trial to the point of task failure. Abdominal and diaphragm contractile function and membrane excitability was assessed 3, 15, and 30 min post-IRL.

Measurements and Procedures

Pulmonary function

Forced vital capacity (FVC), forced expiratory volume in 1 second (FEV_1), FEV_1/FVC , and peak expiratory flow (PEF) were measured using a portable spirometer (Spirolab II, Medical International Research, Vancouver, BC) according to ATS/ERS guidelines ⁵.

Respiratory pressures

A topical anaesthetic (Xylocaine, 2% Lidocaine Hydrochloride) was applied to subjects' nares prior to insertion of two balloon-tipped catheters (no.47-9005, Ackrad Laboratory, Cranford, NJ). Both catheters were inserted in the stomach and all air was removed from the balloons by having the subject perform a brief Valsalva maneuver while the balloons were open to the atmosphere. A glass syringe was used to inject 1mL of air into the esophageal balloon and 2 mL of air into the gastric balloon ⁶. The esophageal catheter was withdrawn into the esophagus. Placement in the esophagus was indicated by the first negative pressure deflection during a series of sniffs. The catheter was then withdrawn an additional 10 cm to ensure that it was completely in the esophagus. The validity of the esophageal balloon catheter placement was verified using the occlusion technique. The balloon catheters were connected to pressure transducers (Validyne Engineering, Model MP45) and calibrated using a Sphygmomanometer (Almedic, Palm Model). P_{di} was calculated by subtracting P_{es} from P_{ga} . P_{di} , P_{ga} , and P_{es} were measured throughout quiet breathing, IRL, and both thoracic and phrenic nerve stimulations. Mouth pressure (P_m) was also monitored by connecting tubing from a side port in the mouth piece to a pressure transducer calibrated across the physiological range. Five MIP maneuvers and MEP maneuvers were performed at baseline and the average of the three best maneuvers was defined as the MIP and MEP for that subject. Both MIP and MEP maneuvers were performed against a device that incorporated a 2 mm orifice to prevent glottic closure. MIP maneuvers were initiated from

functional residual capacity (FRC) and MEP maneuvers were initiated from total lung capacity (TLC). The MIP and MEP values for each subject were compared to predicted values using predictive equations for male MIP and MEP values³³. P_m was also monitored throughout the IRL protocol.

Magnetic stimulation of the diaphragm

Both phrenic nerves were stimulated using a hand held, 90-mm circular coil attached to a magnetic stimulator (Magstim, Magstim 200 Mono Pulse). Subjects sat upright with their necks flexed and the coil was placed between the 5th and 7th cervical vertebrae over the midline. The vertebral level that when stimulated resulted in the highest $P_{di,tw}$ was marked and the coil was positioned at that level for all subsequent stimulations. P_{es} was monitored to ensure that all stimulations were delivered at FRC.

Magnetic stimulation of the abdominals

Subjects sat with their hips flexed and their chest supported by a workout bench inclined 20 degrees from vertical. Once in position, the thoracic nerve roots were stimulated between thoracic vertebrae 8 and 11 (T8 and T11) using a 90-mm circular coil attached to a magnetic stimulator. The vertebral level that when stimulated resulted in the highest $P_{ga,tw}$ was marked and the coil was then positioned at that level for all subsequent stimulations. All stimulations were delivered at FRC by monitoring P_{es} .

Electromyography

Surface electrodes (Kendall H59P Cloth Electrodes) were used to measure electrical activity of the diaphragm, EO, and RA. Electrodes were placed between the 6th and the 8th intercostal space for the diaphragm, ~ 3 cm lateral and ~7 cm superior to the umbilicus for the

RA, and ~15 cm lateral to the umbilicus for the EO. Electrode position varied slightly to ensure optimal M-wave amplitude and areas for all subjects. EMG signals were amplified, band-pass filtered and the analog signals were A/D converted (PowerLab/16SP model ML 795, ADI, Colorado Springs, CO) and recorded using PowerLab data acquisition software (Chart v5.3, ADInstruments, Colorado Springs, CO).

Consistent stimulation

The ability of the magnetic stimulator to consistently activate the muscles of interest (diaphragm, RA, EO) was assessed by creating recruitment curves for each muscle. The stimulator was charged to pre-determined percentages of its maximal output (60, 70, 80, 85, 90, 95 and 100%) and three stimulations, separated by 30 sec to avoid twitch potentiation, were delivered to each of the muscles at each power setting²⁵.

Contractile function and membrane excitability

Contractile function and membrane excitability was assessed before and ~3, 15, and 30 min post-IRL. Abdominal muscle function was assessed prior to diaphragm function at all time points. The twitch protocol consisted of 6 1-Hz potentiated twitches for both the abdominals and diaphragm. When the level of fatigue is low, which we anticipated for the abdominal muscles post-IRL, potentiated twitches provide a more accurate measure of fatigue than unpotentiated twitches³⁴. Abdominal muscle output was assessed by measuring the $P_{ga,tw}$ evoked by 1-Hz stimulations of the thoracic nerve roots after a maximal expiratory effort, ~5 sec in duration, was performed from TLC against a semi-occluded airway. For diaphragm output, $P_{ga,tw}$, and $P_{es,tw}$ were measured in response to 1-Hz stimulations of the phrenic nerve roots after a ~5 sec maximal inspiratory maneuver initiated from FRC and maintained against a semi-occluded airway. $P_{di,tw}$ was obtained by subtraction of $P_{es,tw}$ from $P_{ga,tw}$. All stimulations were delivered at

100% of the stimulator's power output and initiated at the same lung volume (FRC) as judged by non-significant changes in P_{es} .

Reproducibility of twitch pressures

The between-day reproducibility of $P_{ga,tw}$ ramp and baseline values was measured in Subject 1, 5, and 9. Within-day reproducibility of baseline $P_{ga,tw}$ values was measured in Subject 1. The between-day reproducibility of $P_{di,tw}$ ramp and baseline values was measured in Subject 5 and Subject 9.

Inspiratory resistive loading

Subjects performed IRL by inspiring against a flow resistor until task failure. A mouthpiece with separate inspiratory and expiratory ports was used. The inspiratory port consisted of a narrow aperture and the expiratory port was completely unimpeded. During IRL, inspiratory pressure was maintained at 60% of the subject's maximum, inspiratory duty cycle (T_I/T_{TOT}) at 0.7, and breathing frequency (F_b) at 15 breaths/min. To avoid the use of abdominal muscles for postural support, loaded breathing was performed in the supine position. A screen was placed above the subjects during the loading protocol to allow them to see in real time the target inspiratory pressure as well as the inspiratory pressure that they generated with each breath. To ensure the target duty cycle and breathing frequency were maintained, a metronome with distinct inspiratory and expiratory tones was used. Inspired and expired flows were measured using separate pneumotachographs throughout IRL. Blood pressure and HR were measured beat by beat using a Finometer (Finapres Medical Systems, Finometer Model-1). Loading was continued to the point of task failure, which was defined as the point at which the subject could not achieve or maintain the target P_m despite verbal encouragement. P_{ETCO_2} was

measured (VacuMed, Model 17630) throughout the IRL protocol and CO₂ was added to the inspiratory circuit as needed.

Data collection and processing

Raw data (flow, pressure, volume, EMG) was recorded at 10,000 Hz continuously using a 16 channel analog-to-digital data acquisition system (PowerLab/16SP model ML 795, ADInstrument, Colorado Springs, CO) and stored on a personal computer for analysis.

Data Analysis

Consistent stimulation

Average values for diaphragm M-wave amplitude and area in response to phrenic stimulation, and EO and RA M-wave amplitude and area in response to thoracic stimulation were determined for each percentage of the stimulator's power output. M-wave amplitudes were measured from peak-to-peak (mV). M-wave area was calculated by integrating both the positive and negative portions of the action potential. The amplitude of the P_{di,tw} and P_{ga,tw} were measured from baseline to peak for each percentage of the stimulator's power output.

Contractile function and membrane excitability

Average amplitudes of P_{ga,tw} and P_{di,tw} were calculated at each time point for each subject. Fatigue was considered present if there was a greater than 15% reduction in P_{di,tw} or P_{ga,tw} after IRL compared to pre-IRL values³⁵. To ensure consistent degrees of potentiation, the first two twitches at each time point were discarded. Average amplitude and area of the diaphragm, EO, and RA M-waves were determined for each subject at each time point. Pre- to post-IRL percent changes in abdominal and diaphragm contractility were related to the cumulative force output of the muscles to investigate if the degree of fatigue measured is related to force output.

Respiratory and cardiovascular variables during IRL

Tidal P_{ga} and P_{di} swings were calculated for each breath of the IRL trial and averaged over 1 min intervals. P_{di} was integrated over the period of inspiratory flow for each breath during the IRL trial to obtain the diaphragm pressure-time product. The abdominal muscle pressure-time product was calculated by integrating P_{ga} over the period of expiratory flow for each breath during loading. The average tension-time index for the diaphragm (TTI_{di}) was calculated for each min of the IRL trial by multiplying $(P_{di}/P_{di,max}) \cdot (T_I/T_{TOT})$. V_T and F_b for each breath was obtained online by the integration and cyclic measurements of the inspired flow channel, respectively. Minute ventilation (\dot{V}_E) was obtained by online multiplication of V_T and F_b . Systolic (SBP) and diastolic (DBP) pressures were obtained from the beat by beat blood pressure trace and MAP was calculated as $[0.33(SBP-DBP)+DBP]$. Averages for all of the above mentioned variables were calculated for each min of the IRL trial.

Statistical analysis

Friedman repeated measures analysis of variance (ANOVA) on ranks was used to compare the absolute measures of neuromuscular function across time (baseline vs. 3 min post-IRL vs. 15 min post-IRL vs. 30 min post-IRL). Following significant main effects, pairwise comparisons were made using a Tukey post-hoc test. Friedman repeated measures ANOVA on ranks was also used to compare respiratory pressures and physiological variables at equivalent time points during IRL trials. Linear regression analysis was used to determine the relationship between cumulative force output of the diaphragm and the abdominals and the baseline to 3 min post-IRL percent changes in $P_{di,tw}$ and $P_{ga,tw}$, respectively. The acceptable Type I error was set at $P < 0.05$. Results are expressed as mean \pm SE, unless otherwise stated.

Results

Descriptive data

Anthropometric, resting pulmonary function, and respiratory pressure values for all 10 subjects are shown in Table 1. Pulmonary function was similar to predicted values, however, there was considerable variation with values ranging from 78-133% predicted. Average MIP and MEP values were similar to predicted values according to predictive equations for male MIP and MEP³³.

Table 1: Descriptive characteristics of all subjects

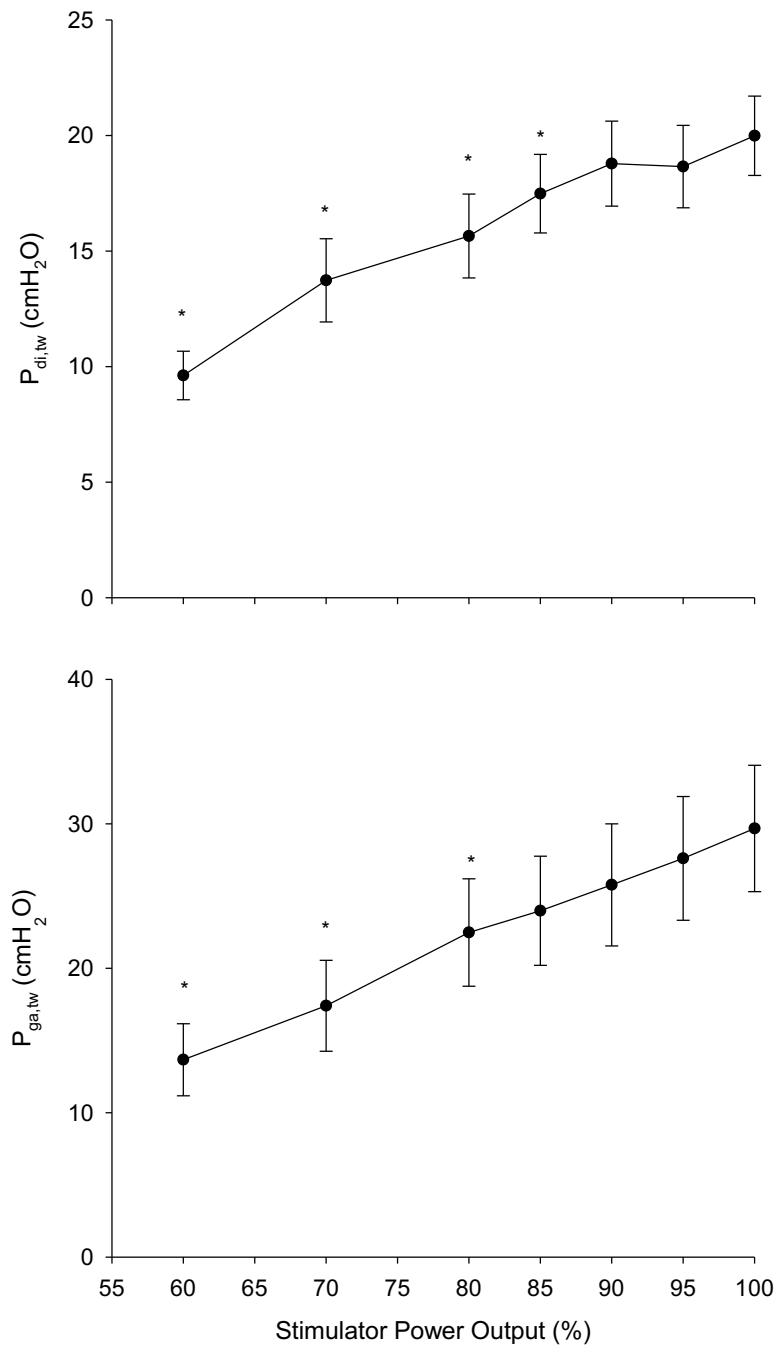
	Value
Height (cm)	180.9 ± 2.5
Weight (kg)	75.9 ± 3.4
Age (years)	25.2 ± 0.9
FVC (L)	5.6 ± 0.3 (102.1 ± 4.3)
FEV ₁ (L)	4.6 ± 0.2 (101.6 ± 3.5)
FEV ₁ /FVC (%)	83.9 ± 1.7 (101.3 ± 2.0)
PEF (L/s)	10.9 ± 0.4 (107.8 ± 4.6)
MIP (cmH ₂ O)	115.6 ± 6.9 (105.3 ± 6.0)
MEP (cmH ₂ O)	126.3 ± 9.3 (82.5 ± 6.1)
P _{diMAX} (cmH ₂ O)	118.7 ± 6.5
P _{gaMAX} (cmH ₂ O)	150.6 ± 5.8

Legend: Values are means ± SE. Values in brackets are percent predicted values for pulmonary function variables. FVC, forced vital capacity; FEV₁, forced expiratory volume in 1 s; PEF, peak expiratory flow; MIP, maximal inspiratory pressure; MEP, maximal expiratory pressure; P_{diMAX}, maximal transdiaphragmatic pressure; P_{gaMAX}, maximal gastric pressure.

Consistent stimulation

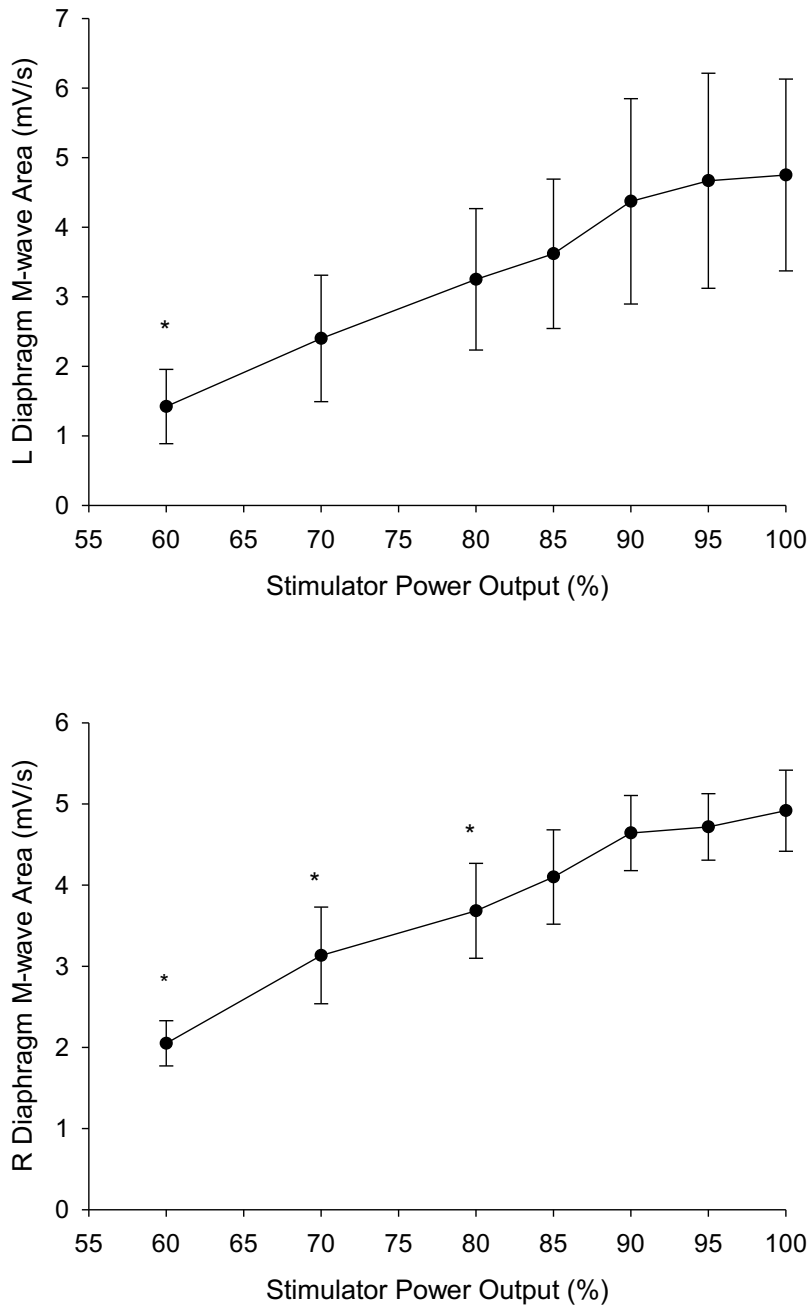
The ramp protocol for $P_{di,tw}$ is shown in Figure 1. Group mean values for $P_{di,tw}$ leveled off at 85% of the stimulator's maximum power output from a statistical perspective, but a clear plateau in pressure was not observed. Left diaphragm M-wave area (Figure 2) and amplitude (Figure 3) were not significantly lower at 80% than at 100% stimulator output. However, no distinct plateau was visible in left diaphragm M-wave amplitude and a clear plateau was not visible until 95% power output for left diaphragm M-wave area. Right diaphragm M-wave area (Figure 2) and amplitude (Figure 3) both leveled off beyond 85% stimulator power output. The ramp protocol for $P_{ga,tw}$ is shown in Figure 1. Mean values for $P_{ga,tw}$ at 85% power output were not significantly lower than values at 100% output; however, an upward trend in pressure continued beyond 85% power output. A leveling off in RA area (Figure 4) and amplitude (Figure 5) was visible beyond 90% stimulator power output. There was clear plateau in EO amplitude (Figure 5), but not EO area (Figure 4) as stimulation intensity increased to 100%.

Figure 1: Group mean transdiaphragmatic twitch pressure and gastric twitch pressure in response to 1-Hz magnetic stimulation of increasing stimulation intensity.



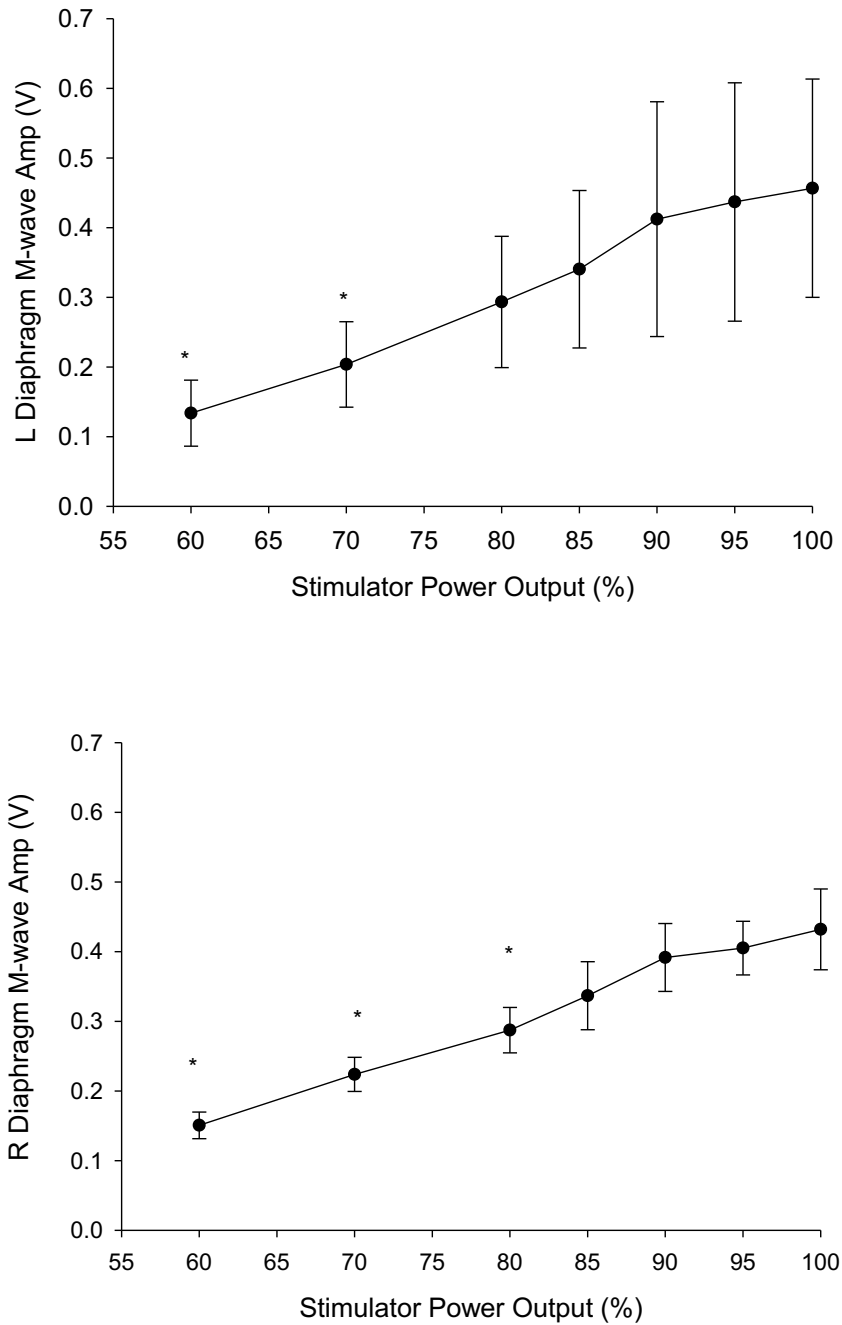
Legend: Values are means \pm SE. *, group mean values are significantly lower from those at 100% of the stimulator's power output ($P < 0.05$).

Figure 2: Left and right diaphragm M-wave area in response to 1-Hz magnetic stimulation of increasing stimulation intensity.



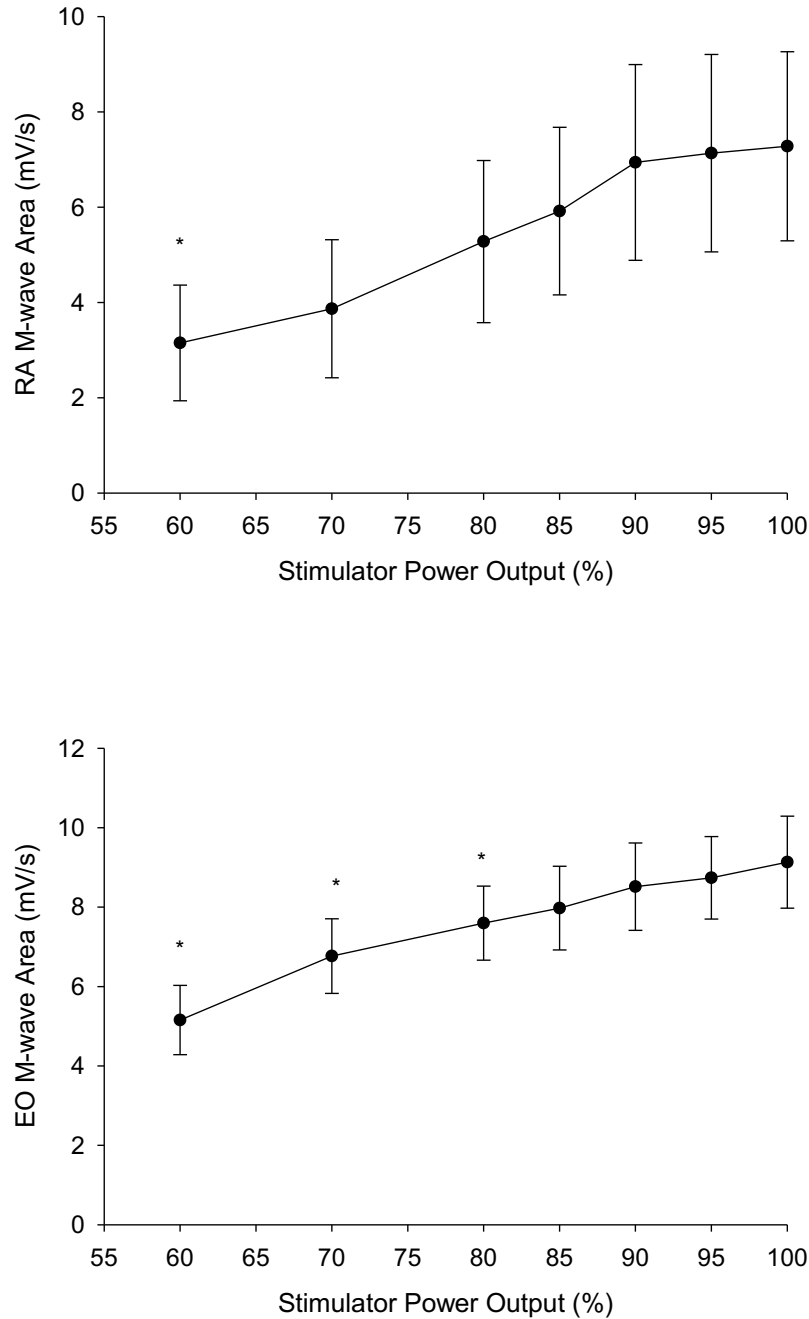
Legend: Values are means \pm SE for 4 subjects. *, group mean values are significantly lower from those at 100% of the stimulator's power output ($P < 0.05$).

Figure 3: Left and right diaphragm M-wave amplitude in response to 1-Hz magnetic stimulation of increasing stimulation intensity.



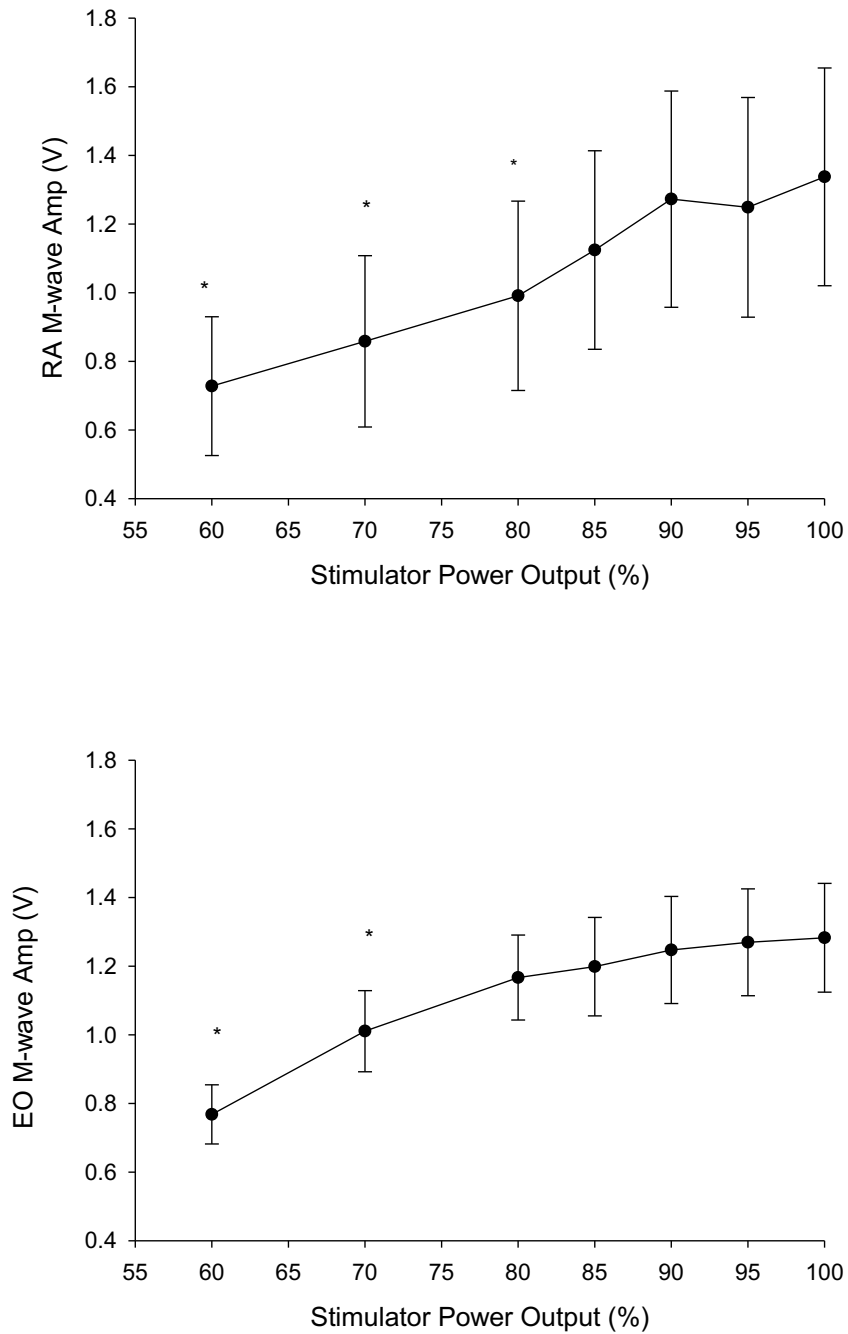
Legend: Values are means \pm SE for 4 subjects. *, group mean values are significantly lower from those at 100% of the stimulator's power output ($P < 0.05$).

Figure 4: Rectus abdominis and external oblique M-wave area in response to 1-Hz magnetic stimulation of increasing stimulation intensity.



Legend: Values are means \pm SE. RA, rectus abdominis; EO, external oblique. Note that RA values are mean data for 6 subjects and EO values are mean data for 9 subjects. *, group mean values are significantly lower from those at 100% of the stimulator's power output ($P < 0.05$).

Figure 5: Rectus abdominis and external oblique M-wave amplitude in response to 1-Hz magnetic stimulation of increasing stimulation intensity.



Legend: Values are means \pm SE. RA, rectus abdominis; EO, external oblique. Note that RA values are mean data for 6 subjects and EO values are mean data for 9 subjects. *, group mean values are significantly lower from those at 100% of the stimulator's power output ($P < 0.05$).

Inspiratory resistive loading

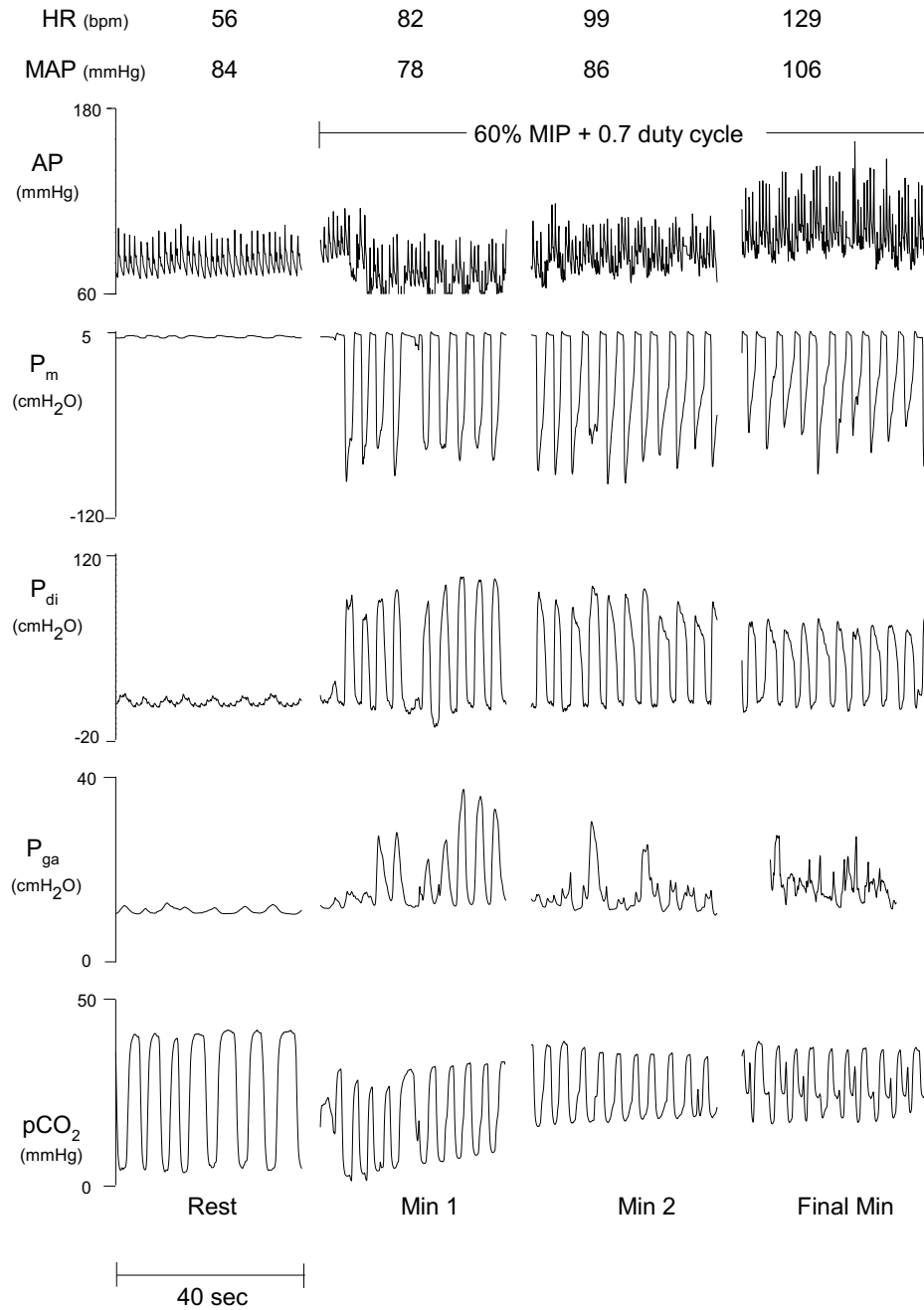
Task failure occurred at 11.9 ± 2.9 min (range=6.8-23.0 min) during the IRL protocol with subjects maintaining T_I/T_{TOT} at 89% of the target value (Table 2). Figure 6 shows raw data from a representative subject during rest, 1st min, 2nd min, and final min of loading and demonstrates how the main respiratory and cardiovascular variables responded during IRL. Cardiovascular variables for this subject are shown along the top of Figure 6, with average HR and MAP values shown above the raw trace of arterial blood pressure (AP). Similar to this representative subject, group mean values for MAP and HR increased in a time dependent manner and mean values for both were not significantly higher than rest until the 4th min of loading. (Table 2, Figure 7). Group average MAP from the 3rd min through to the final min was significantly higher than during the 1st min, further demonstrating the time dependency of increased MAP (Table 2, Figure 7). Respiratory pressure responses for the representative subject are shown in the middle of Figure 6. Similar to the pattern seen in this subject, group mean values of Peak P_{di} and Peak P_{di}/P_{diMAX} steadily declined throughout loading (Table 2). When compared to the first min of loading, both Peak P_{di} and Peak P_{di}/P_{diMAX} during the 6th min and final min were significantly lower (Table 2). Peak P_{ga} , though significantly higher than resting values during the 1st, 2nd, and 4th min, did not contribute substantially to inspiratory pressure generation throughout IRL (Table 2). This can be seen in the raw P_{ga} trace in Figure 6. V_T , F_b , and \dot{V}_E did not vary significantly throughout loading (Table 2). P_{ETCO_2} fell immediately when subjects began inspiring against the resistance. Mean values remained significantly below resting values for the first two min of loading and then increased to within a few mmHg of resting values for the remainder of the trial (Table 2 and Figure 6).

Table 2: Physiological responses during rest, the first 6 min, and final min of loading

	Rest	1 st min	2 nd min	3 rd min	4 th min	5 th min	6 th min	Final min
P _m (cmH ₂ O)	-0.6±0.1	-76.9±4*	-76.6±4*	-76.6±5*	-76.3±4*	-73.5±4	-74.5±4*	-71.6±4*
T _I /T _{TOT}	0.4±0.01	0.6±0.02*	0.6±0.02*	0.6±0.02*	0.6±0.02*	0.6±0.02*	0.6±0.02*	0.6±0.01*
Peak P _{di} (cmH ₂ O)	8.5±1	80.9±4*	75.6±3*	71.8±3*	70.4±2*	71.6±3*	67.8±2 ^s	58.8±2 ^s
P _{di} /P _{diMAX} (%)	7.3±1	69.4±4*	64.6±3*	61.7±3*	60.9±4*	60.8±2*	58.0±2 ^s	50.8±3 ^s
Peak P _{ga} (cmH ₂ O)	2.9±1	18.2±3*	14.1±3*	11.8±2	14.2±3*	14.9±4	12.2±3	9.8±2
P _{ga} /P _{gaMAX} (%)	2±0.4	12±2*	9±1*	8±1	10±2*	10±2	8±2	6±1
V _T (L)	0.8±0.09	2.2±0.2*	2.1±0.2*	2.1±0.2*	2.1±0.2*	2.1±0.2*	2.2±0.2*	2.0±0.1*
F _b (b/min)	14.6±1	16.1±0.2	16.0±0	15.9±0.1	16.3±0.2	16.0±0	16±0.1	16.1±0.1
\dot{V}_E (L/min)	10.7±1	34.9±4*	33.2±4*	33.8±3*	34.0±3*	33.8±3*	34.6±3*	31.7±1*
P _{ETCO₂} (mmHg)	41.7±0.9	31.2±0.8*	36.8±1*	38.4±0.6	38.7±1	39.0±0.4	39.7±0.4	39.7±0.4
HR (bpm)	53.0±3	86.1±7	91.8±7	91.7±8	96.1±7*	97.9±9*	99.7±9*	103±8*
MAP (mmHg)	87.1±3	83.3±2	91.6±3	92.3±4 ^s	97.1±3* ^s	100.6±2* ^s	99.7±3* ^s	99.8±3* ^s

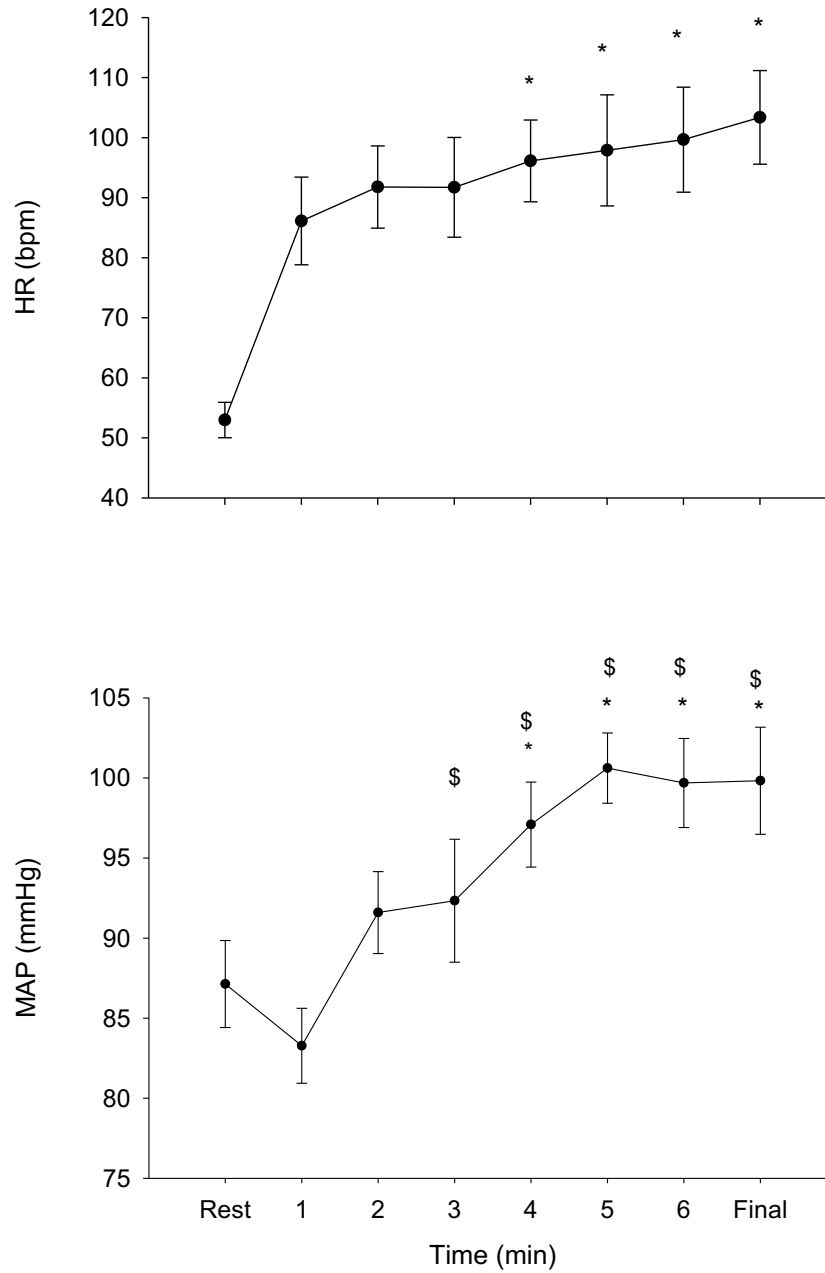
Legend: Values are means ± SE. Note HR and MAP values represent data from 7 of 10 subjects. P_m, mouth pressure; T_I/T_{TOT}, inspired duty cycle; P_{di}, peak transdiaphragmatic pressure; P_{diMAX}, maximal transdiaphragmatic pressure; P_{ga}, peak inspiratory gastric pressure; P_{gaMAX}, maximal gastric pressure; V_T, tidal volume; F_b, breathing frequency; \dot{V}_E , minute ventilation; P_{ETCO₂}, partial pressure of end-tidal carbon dioxide; HR, heart rate; MAP, mean arterial pressure. *, significantly different from rest (p<0.05). ^s, significantly different from 1st min (p<0.05)

Figure 6: Raw data from a representative subject during rest, first min, second min, and final min of inspiratory loading protocol.



Legend: Note the different scales for the three pressure traces. HR, heart rate; MAP, mean arterial blood pressure; MIP, maximum inspiratory mouth pressure; AP, arterial blood pressure; P_m , mouth pressure; P_{di} , transdiaphragmatic pressure; P_{ga} , gastric pressure; PCO₂, partial pressure carbon dioxide.

Figure 7: Heart rate and mean arterial pressure at rest, during the first 6 min, and final min of inspiratory loading protocol

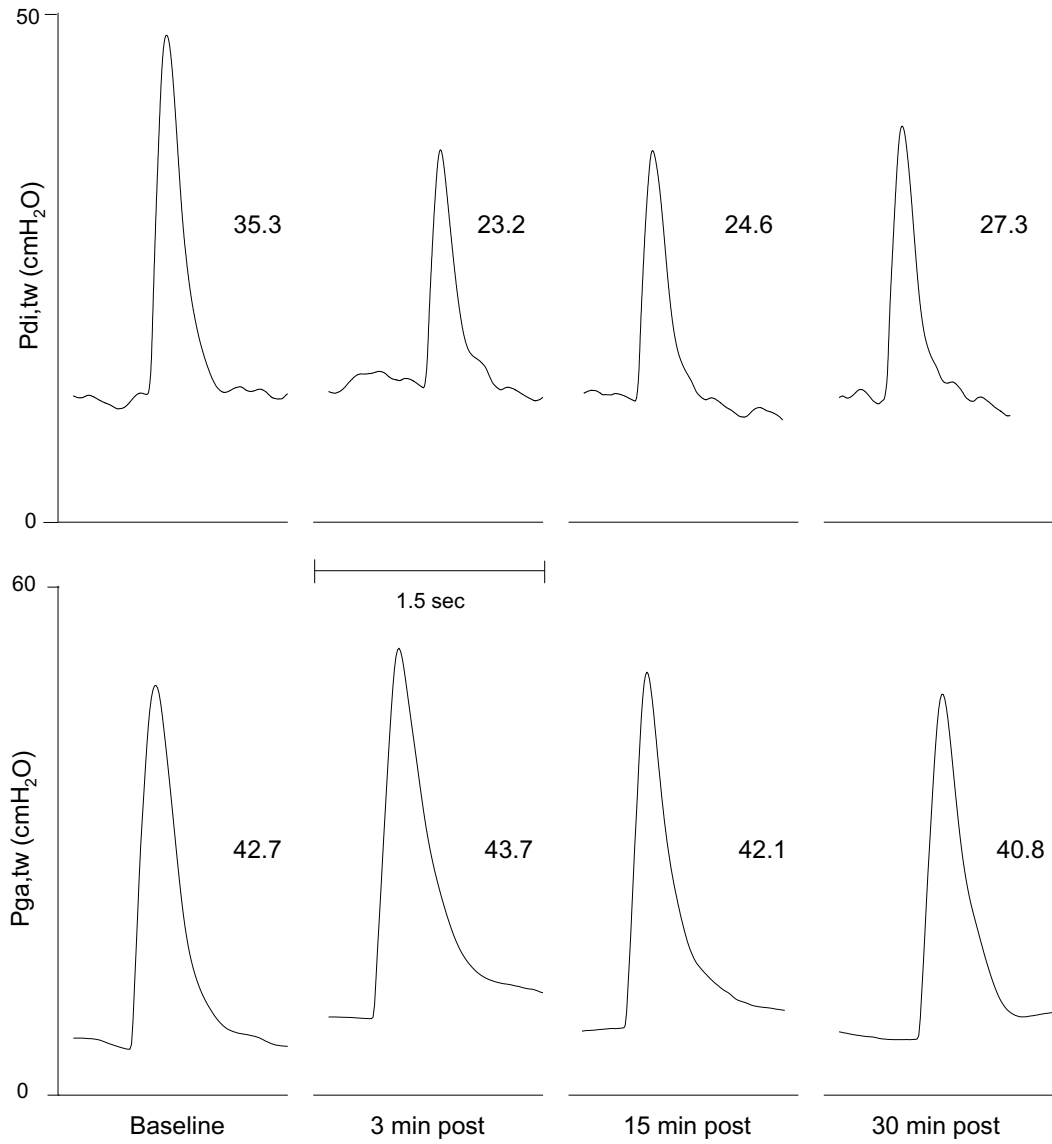


Legend: Values are means \pm SE for 7 subjects. *, significantly different from rest ($p < 0.05$). \$, significantly different from 1st min ($p < 0.05$)

Fatigue

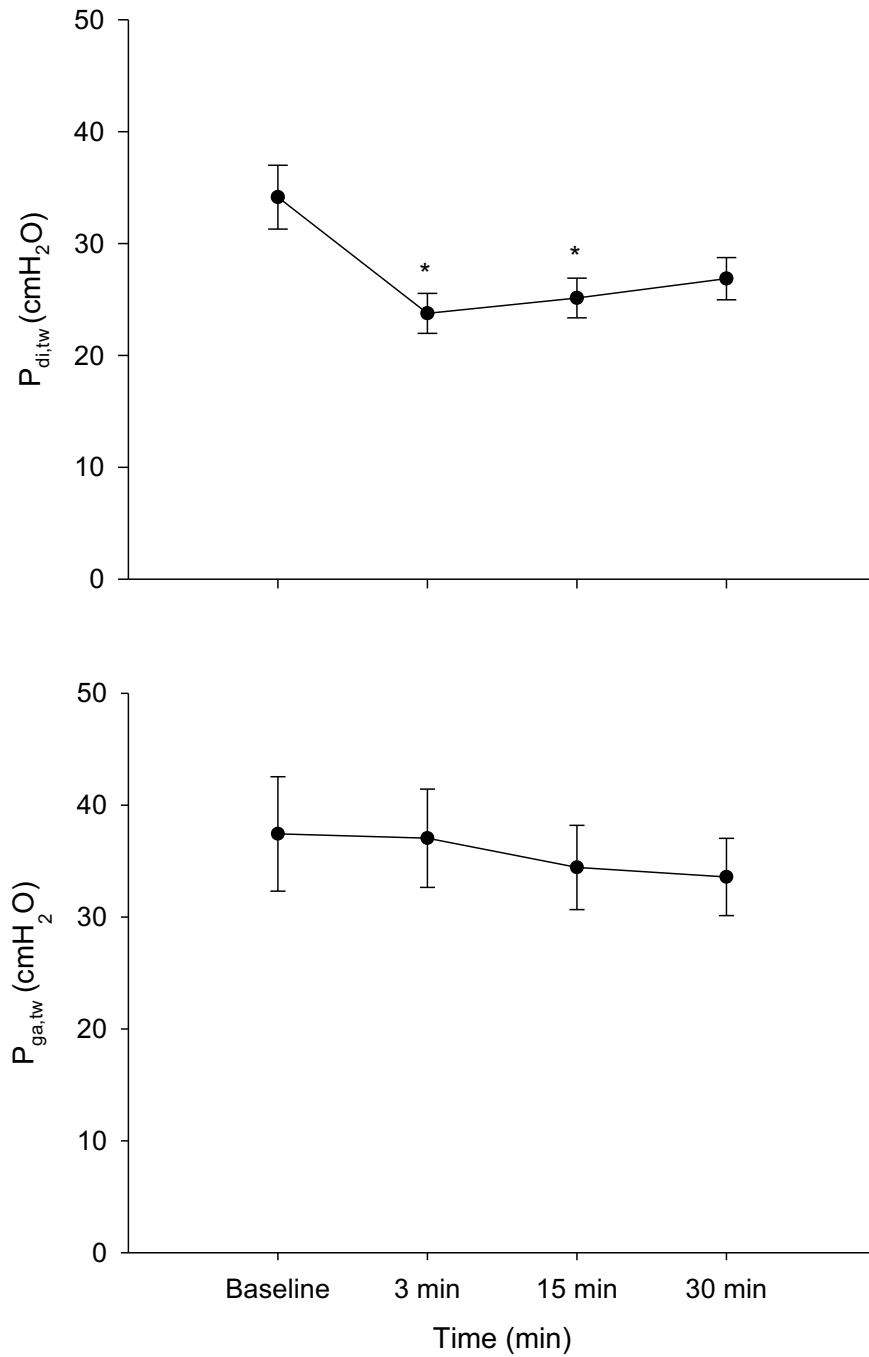
Evoked M-wave amplitudes for the left diaphragm (Figure 12), and RA and EO (Figure 14) did not differ before vs. after IRL. The amplitude of the right diaphragm M-wave was significantly higher 30 min post-IRL than at baseline ($P < 0.05$) (Figure 12). M-wave area for the left and right diaphragm (Figure 11), RA and EO (Figure 13) were not different before vs. after IRL. Figure 8 shows an individual $P_{di,tw}$ and $P_{ga,tw}$ trace at each time point for a representative subject. Absolute $P_{di,tw}$ was significantly lower than baseline (34.1 ± 2.9 cmH₂O) at 3 min post-IRL (23.8 ± 1.8 cmH₂O) and 15 min post-IRL (25.1 ± 1.8 cmH₂O) ($P < 0.05$) (Figure 9). There was no significant difference in baseline and 30 min post-IRL (26.9 ± 1.9 cmH₂O) (Figure 9). The percent change in $P_{di,tw}$ at 3, 15, and 30 min post-IRL was -29.7 ± 2.6 , -25.1 ± 3.5 , $-19.9 \pm 3.6\%$, respectively (Figure 10). $P_{ga,tw}$ did not differ significantly before vs. after IRL (Figure 9). The percent change in $P_{ga,tw}$ at 3, 15, and 30 min post-IRL was 1.2 ± 4.7 , -4.8 ± 4.0 , $-6.8 \pm 3.8\%$, respectively (Figure 10). The cumulative force output of the diaphragm, $\int P_{di}/dt$, was 29307 ± 13784 cmH₂O/s and correlated significantly with the severity of IRL-induced diaphragm fatigue ($r = 0.662$, $P < 0.05$) (Figure 15). IRL-induced abdominal muscle fatigue did not correlate significantly ($r = 0.318$, $P = 0.517$) with the cumulative force output of the abdominals, $\int P_{ga}/dt$ (9470 ± 6493 cmH₂O/s) (Figure 15).

Figure 8: Example of individual transdiaphragmatic and gastric twitch pressure responses to 1-Hz magnetic stimulation at baseline, 3 min post-, 15 min post-, and 30 min post-IRL from a representative subject



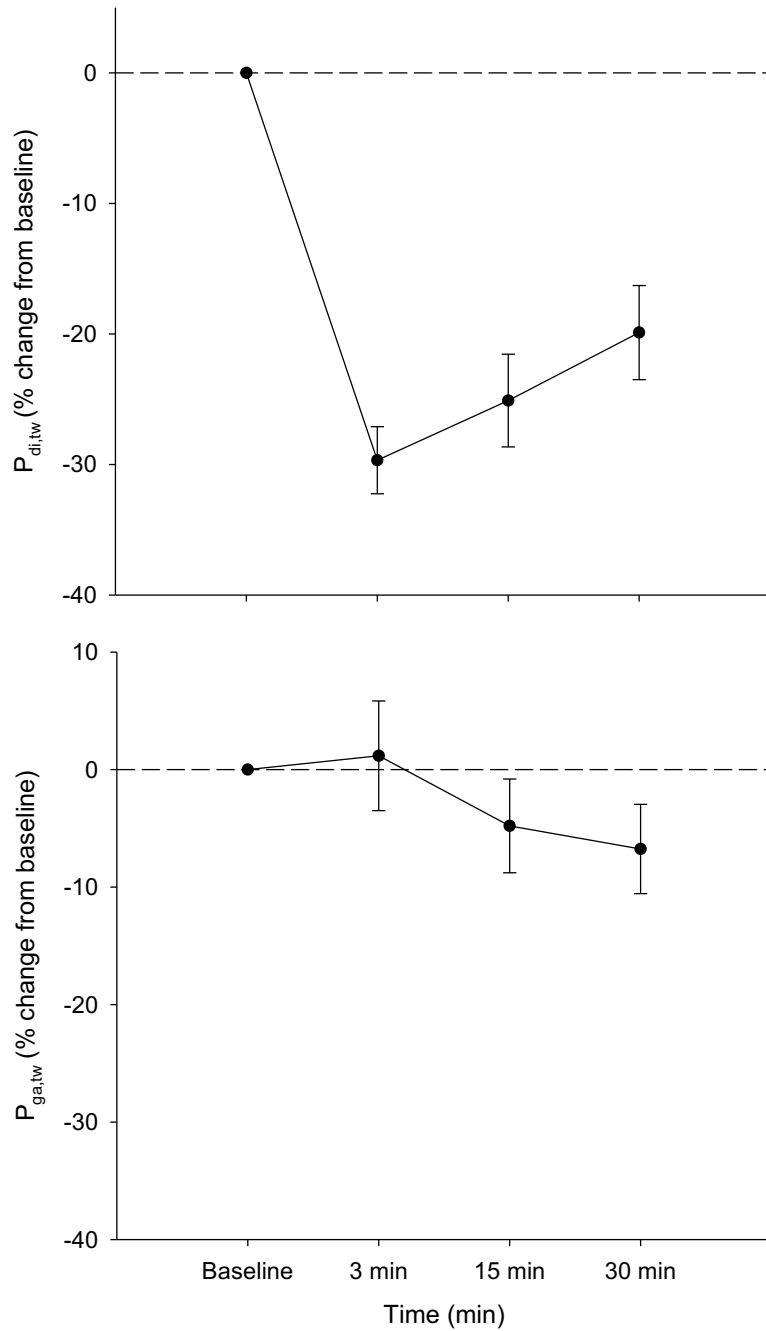
Legend: Values to the right of each individual pressure trace represent the pressure from baseline to peak for that twitch. P_{di,tw}, transdiaphragmatic twitch pressure; P_{ga,tw}, gastric twitch pressure.

Figure 9: Group mean transdiaphragmatic and gastric twitch pressure in response to 1-Hz magnetic stimulation at baseline, 3 min post-, 15 min post-, and 30 min post-IRL.



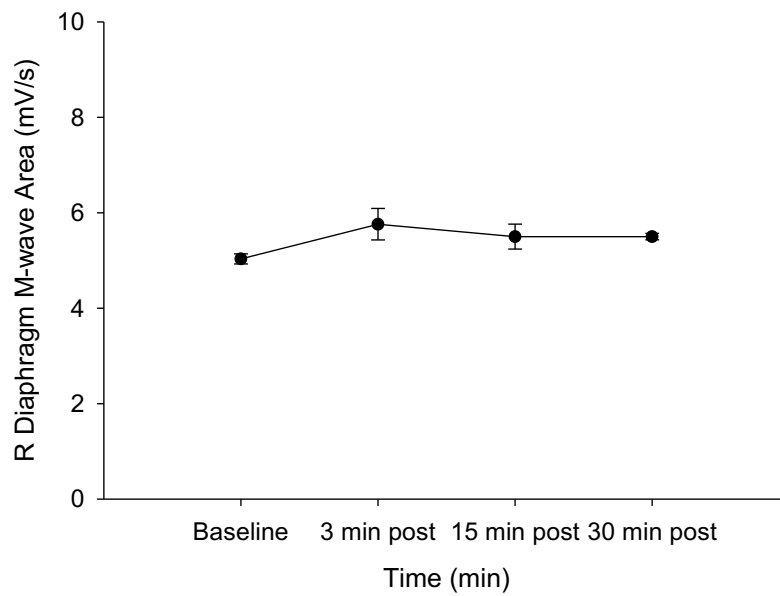
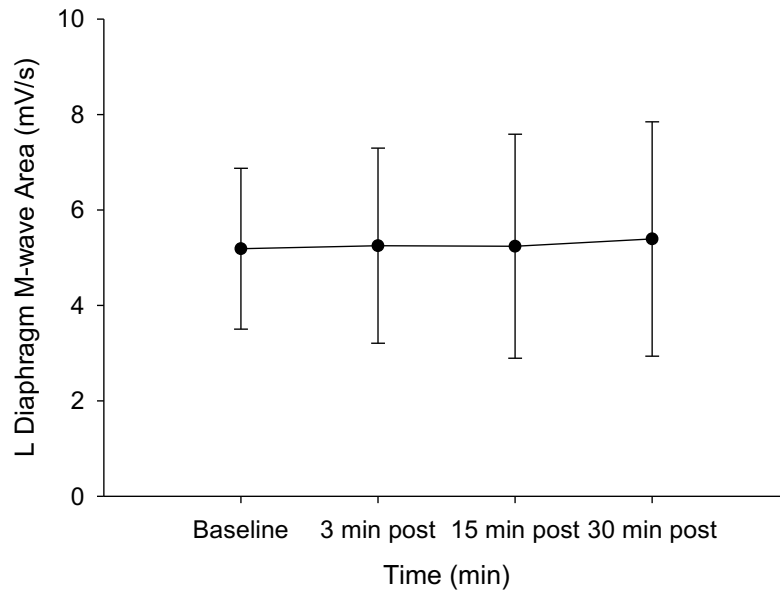
Legend: Values are group means \pm SE. for 10 subjects. P_{di,tw}, transdiaphragmatic twitch pressure; P_{ga,tw}, gastric twitch pressure. *, group mean values significantly different from those at baseline (P<0.05).

Figure 10: Group mean % change from baseline for transdiaphragmatic and gastric twitch pressure in response to 1-Hz magnetic stimulation at baseline, 3 min post-, 15 min post-, and 30 min post-IRL.



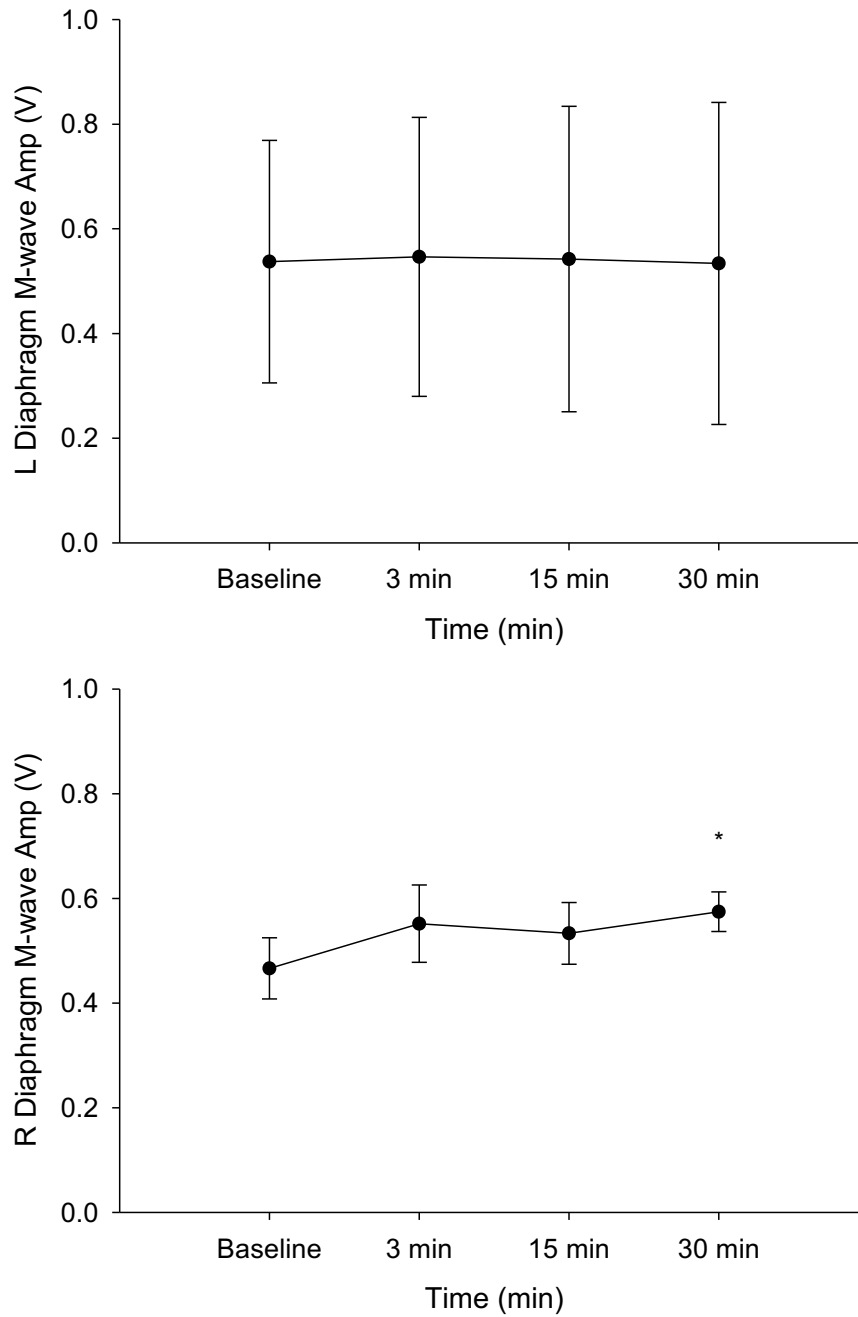
Legend: Values are group means \pm SE. for 10 subjects. $P_{di,tw}$, transdiaphragmatic twitch pressure; $P_{ga,tw}$, gastric twitch pressure. Dashed line represents the baseline.

Figure 11: Left and right diaphragm M-wave area in response to 1-Hz magnetic stimulation at baseline, 3 min post-, 15 min post-, and 30 min post-IRL



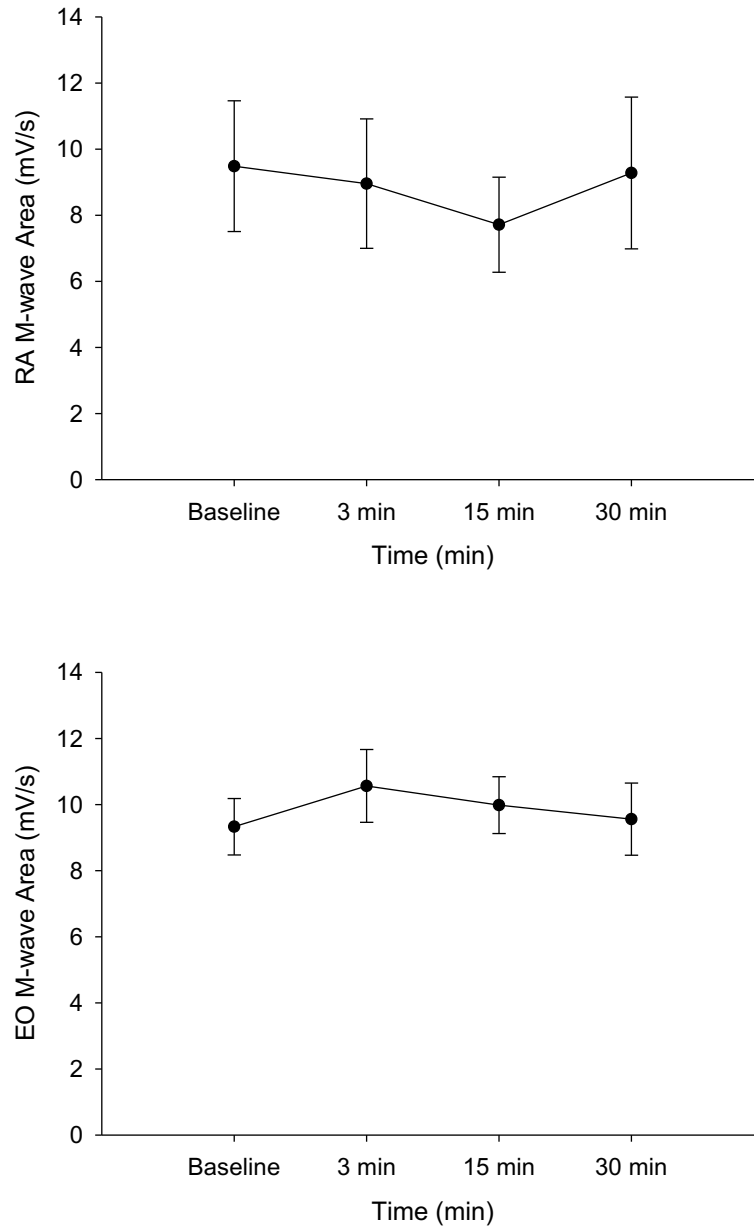
Legend: Values are group means \pm SE. for 4 subjects.

Figure 12: Left and right diaphragm M-wave amplitude in response to 1-Hz magnetic stimulation at baseline, 3 min post-, 15 min post-, and 30 min post-IRL



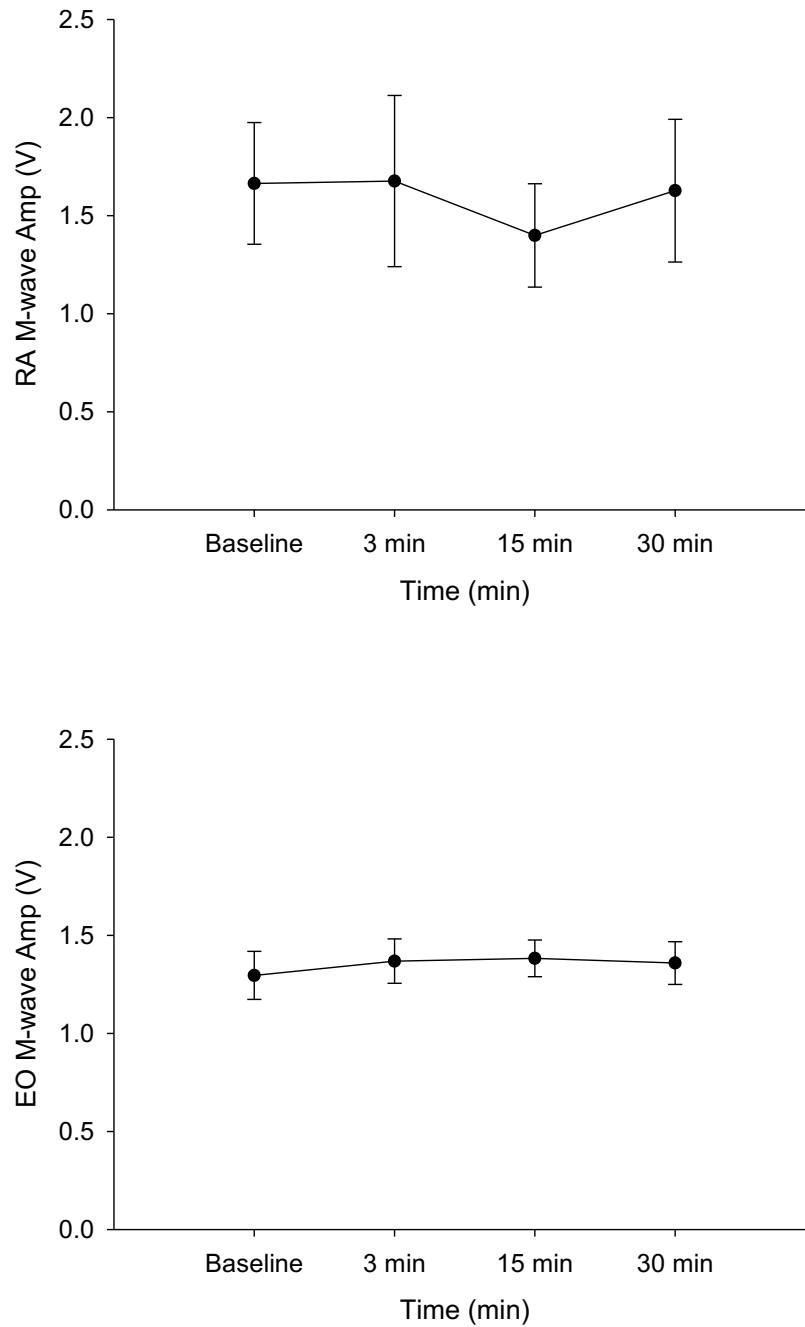
Values are group means \pm SE. for 4 subjects. *, group mean values significantly different from those at baseline ($P<0.05$).

Figure 13: Rectus abdominis and external oblique M-wave area in response to 1-Hz magnetic stimulation at baseline, 3 min post-, 15 min post-, and 30 min post-IRL.



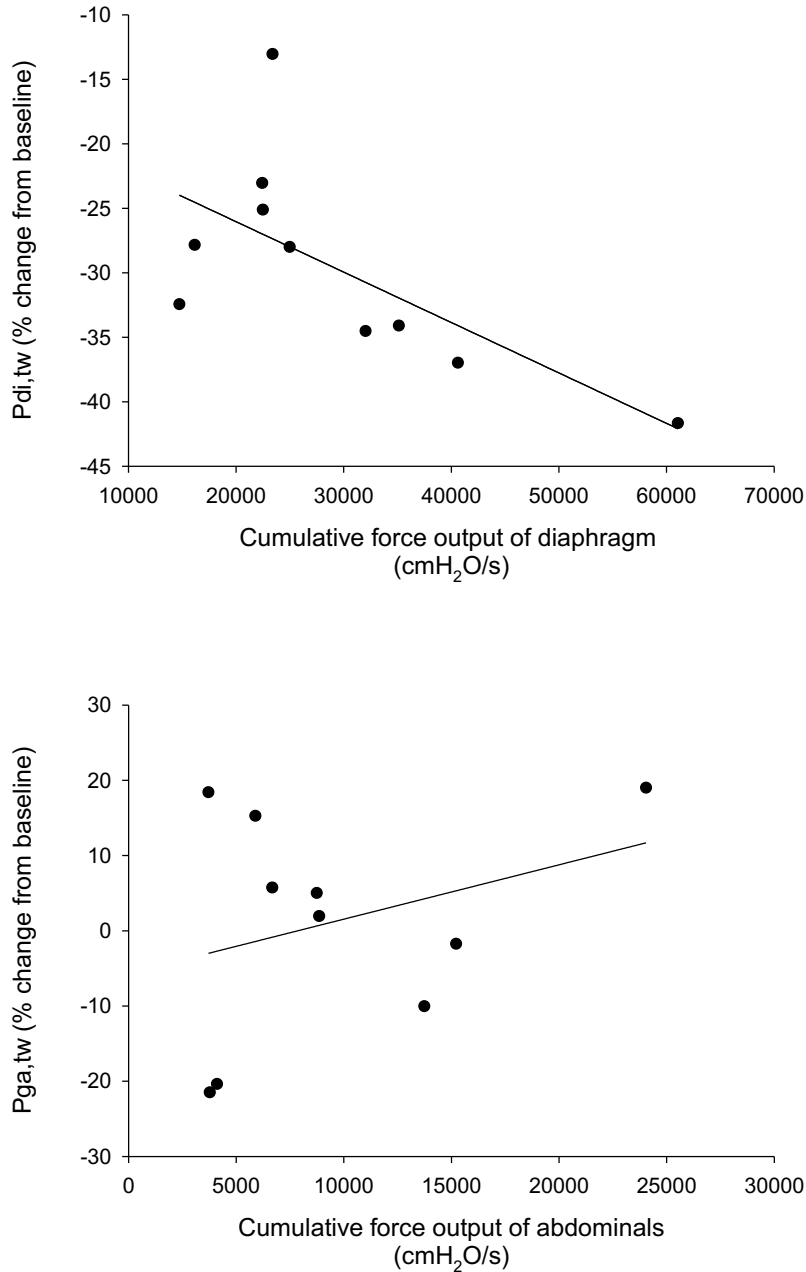
Legend: Values are group means \pm SE. RA, rectus abdominis; EO, external oblique. Note that RA values are mean data for 6 subjects and EO values are mean data for 9 subjects.

Figure 14: Rectus abdominis and external oblique M-wave amplitude in response to 1-Hz magnetic stimulation at baseline, 3 min post-, 15 min post-, and 30 min post-IRL.



Legend: Values are group means \pm SE. RA, rectus abdominis; EO, external oblique. Note that RA values are mean data for 6 subjects and EO values are mean data for 9 subjects.

Figure 15: Relationship between cumulative force output and fatigue of the diaphragm and abdominals for all subjects



Legend: P_{di,tw}, transdiaphragmatic twitch pressure; P_{ga,tw}, gastric twitch pressure. Note that there is a significant correlation between P_{di,tw} and diaphragm force output ($r=0.662$, $r^2=0.439$, $P=0.037$), but not between P_{ga,tw} and abdominal force output ($r=0.318$, $r^2=0.101$, $P=0.517$).

Reproducibility of twitch measures

Subject 1

$P_{ga,tw}$ was variable at 60% during the May 19th trial vs the April 29th trial, with average twitch amplitudes of 18.6 cmH₂O and 13.4 cmH₂O, respectively. By 95% stimulator power output, twitch amplitudes between the trials varied by less than 10% (Table 3). Within-day MEP and P_{gaMAX} during potentiation maneuvers were highly reproducible and $P_{ga,tw}$ varied by only 2.4% between the two sets of baseline measures made during the May 19th trial (Table 4). P_{gaMAX} , MEP, and $P_{ga,tw}$ were lower during the April 29th trial than during the ERL trial, by 19.5%, 6.1%, and 13.0%, respectively (Table 5).

Table 3: Subject 1 between-day gastric twitch ramp reproducibility

Stimulator power output (%)	May 19 th P _{ga,tw} (cmH ₂ O)	April 29 th P _{ga,tw} (cmH ₂ O)	% difference between trials
60	18.3 18.7 18.6	13.9 12.9 13.4	27.9
70	22.1 26.1 26.6	16.1 17.8 18.2	30.3
80	27.3 26.3 26.4	21.8 20.5 20.7	21.2
85	28.5 30.7 29.6	23.1 24.8 24.0	19.1
90	28.5 26.7 28.6	24.4 23.6 26.4	11.4
95	28.5 29.0 30.7	28.4 25.7 26.3	8.7
100	30.6 30.1 30.4	28.9 28.6 27.7	6.4

Legend: Values of the 3 twitches measured at each percentage of the stimulator's power output.
Gastric twitch pressure, P_{ga,tw}

Table 4: Subject 1 within-day reproducibility of baseline gastric twitch

May 19 th 1 st baseline			May 19 th 2 nd baseline		
P _{ga,tw} (cmH ₂ O)	MEP (cmH ₂ O)	P _{gaMAX} (cmH ₂ O)	P _{ga,tw} (cmH ₂ O)	MEP (cmH ₂ O)	P _{gaMAX} (cmH ₂ O)
39.7	103.7	154.2	41.4	97.8	149.0
44.8	101.7	154.7	41.9	108.1	158.4
42.4	95.0	142.5	40.5	105.5	161.1
43.3	108.7	162.6	42.5	95.1	157.6
42.6	102.3	153.5	41.6	101.6	156.5

Legend: Values in bold represent the average value of the 4 pressures above. Gastric twitch pressure, P_{ga,tw}; maximal expiratory pressure, MEP; maximal gastric pressure, P_{gaMAX}

Table 5: Subject 1 between-day reproducibility of baseline gastric twitch

May 19 th			April 29 th		
P _{ga,tw} (cmH ₂ O)	MEP (cmH ₂ O)	P _{gaMAX} (cmH ₂ O)	P _{ga,tw} (cmH ₂ O)	MEP (cmH ₂ O)	P _{gaMAX} (cmH ₂ O)
41.4	97.7	149.0	36.5	87.3	119.6
41.9	108.1	158.4	35.1	99.9	131.0
40.5	105.5	161.1	39.0	100.2	128.0
42.5	95.1	157.6	34.3	94.5	125.2
41.6	101.6	156.5	36.2	95.4	126.0

Legend: Values in bold represent the average value of the 4 pressures above. Gastric twitch pressure, P_{ga,tw}; maximal expiratory pressure, MEP; maximal gastric pressure, P_{gaMAX}

Subject 5

$P_{ga,tw}$ at 100% stimulator power output varied by 18.7% between days (Table 6). P_{gaMAX} , MEP, and $P_{ga,tw}$ during baseline measures were 36.8%, 31.4 %, and 18.7% higher, respectively, during the April 27th trial when compared to the March 30th trial (Table 7). During the ramp protocol for the diaphragm, $P_{di,tw}$ varied by less than 6% between trials above 95% stimulator output (Table 8). Average P_{diMAX} during potentiation MIP maneuvers was 21.4% higher during the March 30th trial than the April 27th trial, despite an 18.8% higher MIP being generated on April 27th (Table 9). $P_{di,tw}$ varied by 26.3% between days (Table 9).

Table 6: Subject 5 between-day gastric twitch ramp reproducibility

Stimulator power output (%)	March 30 th P _{ga,tw} (cmH ₂ O)	April 27 th P _{ga,tw} (cmH ₂ O)	% difference between trials
60	5.5	7.0	15.1
	5.9	6.3	
	5.1	6.3	
70	10.7	8.4	7.4
	8.6	9.0	
	8.0	8.1	
80	10.5	10.0	3.9
	10.2	10.9	
	9.2	10.2	
85	10.3	11.3	18.8
	9.3	13.2	
	10.0	11.9	
90	10.4	12.0	15.8
	10.8	11.6	
	9.2	12.5	
95	10.8	13.7	14.6
	11.1	12.6	
	11.0	12.2	
100	13.1	15.0	18.7
	12.5	16.5	
	13.7	16.8	

Legend: Values of the 3 twitches measured at each percentage of the stimulator's power output.
Gastric twitch pressure, P_{ga,tw}

Table 7: Subject 5 between-day reproducibility of baseline gastric twitch

March 30 th			April 27 th		
P _{ga,tw} (cmH ₂ O)	MEP (cmH ₂ O)	P _{gaMAX} (cmH ₂ O)	P _{ga,tw} (cmH ₂ O)	MEP (cmH ₂ O)	P _{gaMAX} (cmH ₂ O)
15.8	100.0	108.7	21.4	145.0	155.8
17.0	105.6	97.2	20.8	144.6	155.2
17.7	91.8	91.7	21.4	126.	156.2
19.2	89.3	94.8	22.1	147.6	153.5
17.4	96.7	98.1	21.4	141.0	155.2

Legend: Values in bold represent the average value of the 4 pressures above. Gastric twitch pressure, P_{ga,tw}; maximal expiratory pressure, MEP; maximal gastric pressure, P_{gaMAX}

Table 8: Subject 5 between-day transdiaphragmatic twitch ramp reproducibility

Stimulator power output (%)	March 30 th P _{di,tw} (cmH ₂ O)	April 27 th P _{di,tw} (cmH ₂ O)	% difference between trials
60	9.8	7.7	28.2
	9.2	7.8	
	10.8	7.7	
70	14.9	12.4	21.7
	13.6	11.0	
	15.3	12.6	
80	18.9	14.1	22.3
	17.7	15.2	
	18.1	15.5	
85	17.6	18.6	2.4
	18.0	14.7	
	17.0	20.7	
90	16.8	20.5	17.2
	18.4	21.4	
	17.5	21.7	
95	18.0	20.4	4.9
	20.6	20.4	
	19.8	20.5	
100	20.7	21.3	5.2
	19.8	20.5	
	19.6	21.5	

Legend: Values of the 3 twitches measured at each percentage of the stimulator's power output.
Transdiaphragmatic twitch pressure, P_{di,tw}

Table 9: Subject 5 between-day reproducibility of baseline transdiaphragmatic twitch

March 30 th			April 27 th		
$P_{di,tw}$ (cmH ₂ O)	MIP (cmH ₂ O)	P_{diMAX} (cmH ₂ O)	$P_{di,tw}$ (cmH ₂ O)	MIP (cmH ₂ O)	P_{diMAX} (cmH ₂ O)
30.8	-83.4	45.9	22.7	-102.2	33.4
29.6	-83.9	33.9	21.5	-106.4	27.9
31.5	-82.7	41.9	23.9	-100.1	35.5
31.3	-89.8	38.8	22.6	-110.3	29.3
30.8	-85.0	40.1	22.7	-104.7	31.5

Legend: Values in bold represent the average value of the 4 pressures above. Transdiaphragmatic twitch pressure, $P_{di,tw}$; maximal inspiratory pressure, MIP; maximal transdiaphragmatic pressure, P_{diMAX}

Subject 9

$P_{ga,tw}$ at 100% stimulator power output varied by 10.9% between trials, with an average of 35.6 cmH₂O on May 26th and 32.1 cmH₂O on June 30th (Table 10). Average P_{gaMAX} , MEP and $P_{ga,tw}$ baseline values varied by less than 10% between days (Table 11). $P_{di,tw}$ values during the diaphragm ramp protocol were highly variable between the 2 trials. During the May 26th trial, $P_{di,tw}$ at 100% stimulator power output was 38.5% lower than during the June 30th trial (Table 12). P_{diMAX} , MIP, and $P_{di,tw}$ were 14%, 5.3%, and 13.8% higher during the June 30th trial (Table 13).

Table 10: Subject 9 between-day gastric twitch ramp reproducibility

Stimulator power output (%)	May 26 th P _{ga,tw} (cmH ₂ O)	June 30 th P _{ga,tw} (cmH ₂ O)	% difference between trials
60	15.5	21.5	37.7
	11.6	21.4	
	14.9	24.5	
70	16.5	32.5	42.9
	18.4	27.3	
	17.3	31.7	
80	20.9	31.5	29.6
	23.0	33.7	
	28.1	37.1	
85	26.5	39.1	34.1
	23.2	46.1	
	32.2	39.1	
90	31.5	30.9	3.8
	28.3	32.0	
	32.5	33.2	
95	36.3	34.3	10.5
	37.8	33.4	
	31.8	28.1	
100	35.5	33.9	10.9
	35.9	32.0	
	35.3	30.4	

Legend: Values of the 3 twitches measured at each percentage of the stimulator's power output.
Gastric twitch pressure, P_{ga,tw}

Table 11: Subject 9 between-day reproducibility of baseline gastric twitch

May 26 th			June 30 th		
P _{ga,tw} (cmH ₂ O)	MEP (cmH ₂ O)	P _{gaMAX} (cmH ₂ O)	P _{ga,tw} (cmH ₂ O)	MEP (cmH ₂ O)	P _{gaMAX} (cmH ₂ O)
52.5	148.5	151.	42.9	122.7	134.9
46.8	146.1	141.8	49.6	129.	146.9
44.4	128.0	143.6	50.8	127.4	134.0
42.2	130.7	158.4	51.5	128.8	137.0
46.5	138.3	148.8	48.7	127.2	138.2

Legend: Values in bold represent the average value of the 4 pressures above. Gastric twitch pressure, P_{ga,tw}; maximal expiratory pressure, MEP; maximal gastric pressure, P_{gaMAX}

Table 12: Subject 9 between-day transdiaphragmatic twitch ramp reproducibility

Stimulator power output (%)	May 26 th $P_{di,tw}$ (cmH ₂ O)	June 30 th $P_{di,tw}$ (cmH ₂ O)	% difference between trials
60	8.3	7.1	3.9
	6.5	7.5	
	6.9	8.0	
70	8.8	9.7	0.3
	10.6	8.4	
	8.1	9.3	
80	13.8	12.3	9.3
	12.3	9.5	
	10.8	11.9	
85	11.0	14.2	16.1
	13.2	14.7	
	10.1	12.0	
90	14.3	16.6	19.4
	12.3	15.3	
	11.3	15.1	
95	11.2	16.6	33.5
	10.9	16.8	
	11.4	16.9	
100	11.3	19.3	38.5
	13.4	20.1	
	12.4	20.9	

Legend: Values of the 3 twitches measured at each percentage of the stimulator's power output.
Transdiaphragmatic twitch pressure, $P_{di,tw}$

Table 13: Subject 9 between-day reproducibility of baseline transdiaphragmatic twitch

May 26 th			June 30 th		
P _{di,tw} (cmH ₂ O)	MIP (cmH ₂ O)	P _{diMAX} (cmH ₂ O)	P _{di,tw} (cmH ₂ O)	MIP (cmH ₂ O)	P _{diMAX} (cmH ₂ O)
25.6	-112.1	74.2	31.9	-127.5	81.9
32.1	-120.2	70.9	33.1	-127.9	84.1
26.0	-121.9	71.1	29.8	-129.1	82.0
26.7	-124.1	66.5	33.0	-120.6	83.4
27.6	-119.6	70.7	32.0	-126.3	82.8

Legend: Values in bold represent the average value of the 4 pressures above. Transdiaphragmatic twitch pressure, P_{di,tw}; maximal inspiratory pressure, MIP; maximal transdiaphragmatic pressure, P_{diMAX}

Discussion

Major finding

The purpose of this thesis was to determine whether specifically loading the inspiratory muscles caused co-activation of the expiratory abdominals to the point of fatigue. To do this, transdiaphragmatic and abdominal pressure responses to magnetic nerve stimulation were measured before and after subjects completed an IRL protocol known to cause diaphragm fatigue. The major finding of this study is that IRL to the point of diaphragm fatigue and induction of the inspiratory muscle metaboreflex does not co-activate the expiratory abdominal muscles to the point of fatigue. This suggests that IRL elicits reflexive increases in MAP and HR owing to fatiguing contractions of the diaphragm with no contribution coming from abdominal fatigue. That abdominal fatigue is not elicited in response to IRL means that past IRL studies investigating the physiological consequences of inspiratory muscle fatigue can be confident that results were not confounded by abdominal fatigue.

Fatigue

Muscle fatigue can be defined and measured in a multitude of ways³⁶. The definition used for this study is a reduction in force-and/or velocity generating capacity of a muscle that has been under load and is relieved with rest³. In the present study, fatigue of the diaphragm and abdominals was considered present if there was a greater than 15% reduction in $P_{di,tw}$ or $P_{ga,tw}$ in response to magnetic stimulation after IRL compared to pre-IRL values, respectively³⁵. A significant group mean reduction in $P_{di,tw}$ ($-29.7 \pm 2.6\%$; Figure 10) was seen 3 min post-IRL demonstrating that the inspiratory loading protocol utilized was sufficient to cause diaphragm

fatigue. As indicated by non-significant reductions in mean $P_{ga,tw}$, expiratory abdominal muscle fatigue was not present after IRL in this study (Figure 10). This finding does not support the original hypothesis that IRL would co-activate the expiratory abdominal muscles to the point of fatigue.

Abdominal fatigue

Findings from the present study suggest that during IRL the abdominal muscles are not recruited to assist the inspiratory muscles. This contrasts previous findings that suggest co-activation of the abdominal muscles occurs during inspiratory loaded breathing^{26,27}. Activation of the abdominal muscles is thought to occur during inspiratory loading in order to benefit the inspiratory muscles by reducing EELV. At a reduced EELV, increases in V_T occur over the linear portion of the respiratory system compliance curve²⁸ and the diaphragm can function at an optimal length for force development³⁰, whereby storage of elastic energy in the abdominal and thoracic walls aids the subsequent inspiration³¹. In the present study, no reduction in end-expiratory P_{es} during IRL compared to rest was observed, suggesting EELV was not reduced during loading by active recruitment of the abdominals during expiration. Inspiratory abdominal activity, which increases intra-abdominal pressure and provides a fulcrum for diaphragm contraction³⁷, was also minimal throughout IRL. Peak inspiratory P_{ga}/P_{gaMAX} reached a maximum of only $12 \pm 2\%$ during IRL (Table 2).

The lack of abdominal recruitment found in the present study compared to previous studies may be explained by the fact that inspiratory loading in this study was performed in the supine position. The supine position was chosen to avoid activation of abdominal muscles for

postural support³⁸. This position also ensured that results from this study could be compared to previous studies that have investigated the consequences of inspiratory muscle fatigue induced by IRL in the supine position^{11,17,39}. When abdominal muscle recruitment was monitored in both the supine and seated positions, no abdominal EMG activity was seen during IRL in the supine position, but activity was observed in the RA and EO in the seated position²⁶. These findings, coupled with the lack of abdominal fatigue in response to IRL in this study, suggest that body position during loading plays an important role in abdominal muscle recruitment. Abdominal muscle recruitment occurred during IRL in the present study, but the degree of recruitment was minimal. Contractions at submaximal percentages of maximal voluntary force can cause occlusion of blood vessels during isometric contractions⁴⁰, but it is unlikely that P_{ga} during IRL was high enough to limit abdominal muscle blood flow. It is probable that abdominal muscles were consistently perfused during IRL in the supine position and therefore not surprising that no expiratory abdominal fatigue occurred (Figure 9).

Diaphragm fatigue

The relationship between the mean P_{di} developed during inspiration and the fraction of the total breath cycle that inspiration is held has been previously related to the amount of time breathing can be sustained⁴¹. Subjects were tasked with targeting between 15-90% of P_{diMAX} while maintaining T_I/T_{TOT} between 0.15 and 1. The time that each breathing pattern could be sustained was inversely related to P_{di} and T_I/T_{TOT} . Using these results, Bellemare and Grassino (1982) defined the TTI_{di} as:

$$TTI_{di} = (P_{di}/P_{diMAX})(T_I/T_{TOT})$$

When TTI_{di} was 0.15 or less, breathing could be sustained indefinitely. Above this threshold, the time breathing could be sustained decreased as a function of TTI_{di} ⁴¹. The impact that TTI_{di} has on diaphragmatic blood flow was then investigated in an animal model. Diaphragm blood flow was measured in 6 canines by catheterizing a branch of the diaphragmatic vein and counting blood drops with an infrared cell⁴². Using bilateral electrical stimulation of the phrenic nerves, contraction time and the level of tension developed by the canine diaphragms was controlled. During intermittent contractions, those with periods of pressure generation and relaxation, blood flow to the diaphragm was limited above a TTI_{di} of 0.2⁴².

The IRL protocol chosen for this study had subjects target 60% of MIP with a 0.7 T_I/T_{TOT} that would result in a TTI_{di} around 0.4. Previous IRL studies in humans have demonstrated that this protocol does indeed cause fatigue of the diaphragm^{11,17}. In the present study, peak inspiratory P_{di} was increased significantly above resting values throughout IRL, with values ranging from $69.4 \pm 13\%$ P_{diMAX} during the 1st min to $50.8 \pm 10\%$ P_{diMAX} during the final min (Table 2). Although subjects maintained a T_I/T_{TOT} slightly lower than the target value of 0.7, the average TTI_{di} was 0.4 throughout the first 6 min of loading and 0.3 during the final min (Table 2). The relatively high TTI_{di} likely caused a reduction in blood flow to the diaphragm, leading to reduced oxygen delivery and fatigue. Blood flow would have been compromised to a greater extent in subjects that generated the most pressure over time during IRL compared to those that generated the least. This is supported by the fact that the degree to which the diaphragm fatigued correlated significantly with the cumulative force output of the diaphragm during IRL ($P < 0.5$) (Figure 15).

Mechanisms of diaphragm fatigue

M-wave amplitude and area were monitored throughout stimulations to ensure that any reduction in $P_{di,tw}$ or $P_{ga,tw}$ was not due to neuromuscular transmission failure or de-recruitment of muscle fibers. M-wave amplitude and area for both sides of the diaphragm were not significantly lower than baseline at 3 min post-IRL (Figures 11 and 12), when the greatest amount of diaphragm fatigue was measured (Figures 9 and 10). This suggests that reductions in $P_{di,tw}$ were not due to de-recruitment of fibers or transmission failure. Peripheral components of fatigue include sarcolemma excitability, excitation contraction coupling, contractile mechanisms, and metabolic energy supply and accumulation⁴³. The high TTI_{di} and sympathetically-mediated metaboreflex induced increase in HR and MAP (Table 2) suggest metabolic energy supply and accumulation as potential sites of diaphragm fatigue found in this study. Diaphragm fatigue may also have been a reflection of changes in the intracellular calcium transient. The amount of calcium released during a single twitch places the diaphragm on the steep region of the sigmoidal relationship between force and intracellular calcium⁴⁴. This means that a small decline in the amplitude of the intracellular calcium transient elicits a large drop in force. Direct measurements of intracellular calcium have been made in single mammalian fibers which demonstrate that for a given stimulation frequency there was a reduced intracellular calcium concentration in the fatigued fibers⁴⁵. A reduction in amplitude of the intracellular calcium transient released in response to the 1 Hz twitches utilized in this study could have caused the reduction in $P_{di,tw}$ observed post-IRL.

Eliciting the respiratory muscle metaboreflex

Evidence in animals indicates that the diaphragm and other inspiratory and expiratory muscles are richly innervated by mechanoreceptor (Type III) and metaboreceptor (Type IV) nerve afferents^{19,20}. The role played by these afferents during increased diaphragmatic or abdominal pressure production encountered during resistive loading in humans has been previously investigated^{11,17,18,39}. When MSNA was measured in the resting peroneal nerve while subjects inspired at 60% MIP and T_I/T_{TOT} of 0.7, MSNA was unchanged in the first 1-2 min but then increased over time to $77 \pm 51\%$ (S.D.) above rest¹⁷. This same IRL protocol caused a time-dependent increase in HR and MAP^{11,17,39}. The time-dependent increase in MSNA, HR and MAP is attributed to an inspiratory muscle metaboreflex. Accumulating metabolic end products in a fatigued diaphragm, in the face of compromised blood flow due to the high TTI_{di} , cause an increase in sympathetic outflow and a subsequent increase in MAP and HR^{11,17}. A similar metaboreflex occurs during ERL when the expiratory muscles are activated to the point of fatigue. An ERL protocol of 60% MEP and an expiratory duty cycle of 0.7 caused a time dependent increase in MSNA and MAP¹⁸. However, the role of fatiguing contractions of the abdominals played in the metaboreflex that occurred during ERL is hard to quantify, as a recent study demonstrated that both expiratory and inspiratory muscles fatigue in response to ERL¹⁰. This suggests that the increases in MSNA and MAP demonstrated during ERL could have been the result of the fatigued diaphragm eliciting the inspiratory muscle metaboreflex.

The increased P_{di} associated with the IRL protocol used in this study likely caused mechanical deformation of the diaphragm and increased the activity of the mechanically sensitive (type III) afferent fibers within this muscle⁴⁶. The metabolically sensitive (type IV)

afferent fibers were likely stimulated by an accumulation of lactic acid, inorganic phosphates, and other metabolic by-products leading to a sympathetically mediated metaboreflex⁴⁷. The time-dependent nature of the increase in HR and MAP observed in this study (Table 2) are consistent with previous IRL studies^{11,17,39}. No objective evidence of abdominal muscle fatigue was found in this study (Figure 9 and 10), suggesting the reflexive increases in MAP and HR in were due to fatiguing contractions of the diaphragm with no contribution coming from abdominal fatigue¹⁸.

End-tidal CO₂ during IRL

Previous IRL studies have found that task failure is not always associated with inspiratory muscle fatigue^{48,49}. When subjects were tasked with inspiring against resistive loads ranging from 35-90% of MIP for 20 min, task failure occurred before the 20 min mark in all subjects at higher loads (75-90% MIP)⁴⁸. MIP measured post-IRL in all trials in which task failure occurred before 20 min was not lower than MIP measured at baseline (MIP increased from 90.2 ± 13.6 to $101.6 \pm 17\%$ of pretrial MIP) and $P_{di,tw}$ also showed no decline post-IRL vs baseline (initial 27.5 ± 15.6 cmH₂O; final 29.4 ± 13.3 cmH₂O)⁴⁸. $P_{ET}CO_2$ rose by $1.6 \pm 0.9\%$ in task failure trials and subjects reported close to maximal levels of dyspnea on the Borg scale in these trials⁴⁸. These data suggest that task failure was associated with hypercapnia and dyspnea, not muscle fatigue. Even when rib cage and diaphragm fatigue is detected after IRL, the degree of muscle fatigue is not always related to the duration that loaded breathing can be sustained⁵⁰. This suggests that other factors, such as CO₂ accumulation and a decrease in arterial oxygen saturation, probably caused task failure⁵⁰. In the present study, $P_{ET}CO_2$ was monitored during resting breathing and

throughout the duration of each IRL trial. Mean values during the 1st and 2nd min of IRL (31.2 ± 3 and 36.8 ± 4) were significantly lower than those at rest (41.7 ± 3); however, values during the 3rd to final min were not significantly different from rest (Table 2). We can be confident that task failure was not related to CO₂ accumulation in this study due to the maintenance of P_{ET}CO₂ close to resting values from the 3rd to final min of loading.

Reproducibility of twitch measures

In subject 1, the between-day reproducibility of P_{ga,tw} ramp data and both the within- and between-day reproducibility of P_{ga,tw} baseline data were measured. Previous within-day measures of P_{ga,tw}, made in 7 male subjects with the same stimulation protocol used in the current study, averaged 40.4 cmH₂O during the 1st set of twitches and 41.1 cmH₂O during the 2nd set completed 30 minutes later²⁵. Consistent with previous findings, the within-day P_{ga,tw} values for Subject 1 in this study were very consistent. P_{ga,tw} averaged 42.6 cmH₂O during the 1st set of baseline twitches, and averaged 41.6 cmH₂O during the second set (Table 4). The variability in P_{ga,tw} baseline measures in Subject 1 on separate days was likely due to differences in the degree of potentiation from one day to the next (Table 5). The strength of the voluntary contraction during potentiation efforts prior to nerve stimulation is known to effect the amplitude of the muscle twitch⁵¹. When P_{di,tw} was measured before and after voluntary contractions of 100%, 75%, 50%, and 25% of P_{diMAX}, P_{di,tw} was significantly increased after 100%, 75%, and 50% contractions⁵¹. The mean percent increase in P_{di,tw} was 41% after a 5 sec voluntary contraction at 75% P_{diMAX} and 47% after a 5 sec contraction at 100% P_{diMAX}⁵¹. In the present study, Subject 1's P_{gaMAX} during the 5 sec potentiation effort was 126.0 cmH₂O during the April 29th trial and 156.5 cmH₂O during the May 19th trial, which resulted in P_{ga,tws} of 36.2 cmH₂O and 41.6 cmH₂O,

respectively (Table 5). These results are consistent with the strength of voluntary contraction during potentiation maneuvers correlating positively with twitch amplitude.

In Subject 5, the thoracic nerve roots were likely stimulated more effectively during the $P_{ga,tw}$ twitch ramp on April 27th than on March 30th, resulting in higher twitch amplitudes (Table 6). The variability in baseline $P_{ga,tw}$ measures between days was likely due to a lack of subject motivation during potentiation efforts on March 30th. During the March 30th trial, the average MEP and P_{gaMAX} values for Subject 5 were 96.7 cmH₂O and 98.1 cmH₂O, respectively. The average MEP achieved on April 27th was 141.0 cmH₂O and P_{gaMAX} was 155.2 cmH₂O on average. Consistent with previous results, the significantly higher pressures generated during potentiation maneuvers resulted in higher $P_{ga,tw}$ on April 27th (Table 7)⁵¹. $P_{di,tw}$ was similar between trials during the diaphragm ramp protocol; however, it is likely that the phrenic nerves were stimulated more effectively during the April 27th trial due to $P_{di,tw}$ being higher in amplitude at 90%, 95%, and 100% stimulator power output (Table 8). Baseline $P_{di,tw}$ was 26.3% lower during the April 27th trial compared to the March 30th trial, despite the 19% increase in MIP that would suggest the diaphragm was potentiated to a greater extent on April 27th (Table 9). The lower $P_{di,tw}$ after a higher MIP can be explained by differences in the extent to which the diaphragm was recruited to generate the inspiratory pressure. Subject 5 generated a higher P_{diMAX} on March 30th by recruiting his diaphragm to a greater extent during MIP maneuvers. This caused a greater potentiation of the diaphragm and resulted in a higher $P_{di,tw}$ (Table 9).

In Subject 9, $P_{ga,tw}$ ramp data was variable both within-day and between days. On June 30th, $P_{ga,tw}$ measured at 85% stimulator output was higher than that at 100% power output. The high level of variability in $P_{ga,tw}$ for this subject suggests that the thoracic nerves were not being consistently stimulated during the abdominal ramp protocol, particularly during the June 30th trial (Table 10). This inconsistency in twitch amplitude was also seen during the potentiated baseline twitches. Average baseline values of $P_{ga,tw}$ varied by only 4.7% between May 26th and June 30th (Table 11), but post-IRL measures of $P_{ga,tw}$ made during the May 26th trial had coefficients of variation as high as 23%. The thoracic nerve roots of Subject 9 could not be consistently stimulated in this study. Table 12 shows the ramp protocol for the diaphragm in Subject 9. The phrenic nerves were stimulated more effectively during the June 30th trial than on the May 26th trial. Average $P_{di,tw}$ was 13.8% lower on May 26th compared to June 30th (Table 13). The difference in $P_{di,tw}$ values can likely be explained by the lower MIP and P_{diMAX} achieved during potentiation of the diaphragm on May 26th (Table 13).

Methodological considerations

Similar to other studies, $P_{di,tw}$ and the diaphragm M-wave amplitudes and areas in response to magnetic stimulation of the phrenic nerves leveled off from a statistical perspective above 85% of stimulator power output^{7,51,52}. However, unlike previous studies, $P_{di,tw}$ and M-wave amplitudes and areas for both sides of the diaphragm continued to trend upward (Figures 1-3). The lack of a distinct plateau during the ramp protocol suggests that the diaphragm may have been stimulated submaximally in some subjects. $P_{ga,tw}$ at 85% of stimulator power output was not statistically lower than values at 100% of stimulator power output, but values continued to trend upward and a clear plateau was not observed (Figure 1). There was also a tendency for RA and

EO area and amplitude to level off but not entirely plateau (except for EO amplitude) (Figures 4 and 5). These data suggest that thoracic stimulation was likely submaximal in the muscles that contribute to $P_{ga,tw}$. Although stimulation of both the phrenic and thoracic nerve roots may have been submaximal in some individuals, several steps were taken to ensure that the degree of stimulation remained consistent throughout the study. All stimulations were delivered at 100% of the stimulator's power output and the coil position for both phrenic and thoracic stimulation was marked before baseline measures were made to ensure that the coil was positioned the same was for all stimulations. End-expiratory P_{es} , utilized as a surrogate for lung volume, was measured before all stimulations and care was taken to avoid stimulating the phrenic nerve when the pressure varied by more than a few cmH_2O . By maintaining a similar lung volume, we hoped to ensure that the length of the diaphragm remained consistent throughout the stimulation protocol to avoid differences in $P_{di,tw}$ due to the length tension relationship of the muscle³⁰. Average values for $P_{di,tw}$ and $P_{ga,tw}$ at baseline were similar to previous studies using cervical magnetic stimulation^{7,25} and thoracic magnetic stimulation²⁵, suggesting both the phrenic and thoracic nerves were stimulated effectively.

Conclusions

IRL elicits objective evidence of diaphragm fatigue, but not abdominal muscle fatigue. The agonist-antagonist interactions of the respiratory muscles previously reported during ERL do not seem to be as important to consider during IRL. These results suggest that future studies attempting to characterize the physiological consequences of diaphragm fatigue, without the confounding effects of abdominal fatigue, can use IRL to induce diaphragm fatigue.

References

1. Johnson, B. D., Babcock, M. A., Suman, O. E. & Dempsey, J. A. Exercise-induced diaphragmatic fatigue in healthy humans. *J. Physiol.* **460**, 385–405 (1993).
2. Taylor, B. J., How, S. C. & Romer, L. M. Exercise-induced abdominal muscle fatigue in healthy humans. *J. Appl. Physiol.* **100**, 1554–1562 (2006).
3. NHLBI Workshop summary. Respiratory muscle fatigue: report of the respiratory muscle fatigue workshop group. *Am. Rev. Respir. Dis.* **142**, 474–80 (1990).
4. Bellemare, F. & Bigland-Ritchie, B. Assessment of human diaphragm strength and activation using phrenic nerve stimulation. *Respir. Physiol.* **58**, 263–277 (1984).
5. ATS/ERS. Statement on respiratory muscle testing. *Am J Respir Crit Care Med* **166**, 518–624 (2002).
6. Milic-Emili, J., Mead, J., Turner, J. M. & Glauser, E. M. Improved technique for estimating pleural pressure from esophageal balloons. *J. Appl. Physiol.* **19**, 207–11 (1964).
7. Similowski, T. *et al.* Cervical magnetic stimulation: a new painless method for bilateral phrenic nerve stimulation in conscious humans. *J. Appl. Physiol.* **67**, 1311–1318 (1989).
8. Aubier, M., Farkas, G., De Troyer, A., Mozes, R. & Roussos, C. Detection of diaphragmatic fatigue in man by phrenic stimulation. *J. Appl. Physiol.* **50**, 538–44 (1981).
9. Kyroussis, D. *et al.* Simulation of cough in man by magnetic stimulation of the thoracic nerve roots. *Am. J. Respir. Crit. Care Med.* **156**, 1696–1699 (1997).
10. Taylor, B. J. & Romer, L. M. Effect of expiratory muscle fatigue on exercise tolerance and locomotor muscle fatigue in healthy humans. *J. Appl. Physiol.* **104**, 1442–51 (2008).
11. Sheel, A. W. *et al.* Fatiguing inspiratory muscle work causes reflex reduction in resting leg blood flow in humans. *J. Physiol.* **537**, 277–289 (2001).
12. Supinski, G. S., Clary, S. J., Bark, H. & Kelsen, S. G. Effect of inspiratory muscle fatigue on perception of effort during loaded breathing. *J. Appl. Physiol.* **62**, 300–7 (1987).

13. Chonan, T., Altose, M. D. & Cherniack, N. S. Effects of expiratory resistive loading on the sensation of dyspnea. *J. Appl. Physiol.* **69**, 91–5 (1990).
14. Suzuki, S., Suzuki, J., Ishii, T., Akahori, T. & Okubo, T. Relationship of respiratory effort sensation to expiratory muscle fatigue during expiratory threshold loading. *Am. Rev. Respir. Dis.* **145**, 461–6 (1992).
15. Mador, M. J. & Acevedo, F.A. Effect of respiratory muscle fatigue on subsequent exercise performance. *J. Appl. Physiol.* **70**, 2059–2065 (1991).
16. Verges, S., Sager, Y., Erni, C. & Spengler, C. M. Expiratory muscle fatigue impairs exercise performance. *Eur. J. Appl. Physiol.* **101**, 225–232 (2007).
17. St Croix, C. M., Morgan, B. J., Wetter, T. J. & Dempsey, J. A. Fatiguing inspiratory muscle work causes reflex sympathetic activation in humans. *J. Physiol.* **529 Pt 2**, 493–504 (2000).
18. Derchak, P. A., Sheel, A. W., Morgan, B. J. & Dempsey, J. A. Effects of expiratory muscle work on muscle sympathetic nerve activity. *J Appl Physiol* **92**, 1539–1552 (2002).
19. Duron, B. in *Regulation of Breathing, Part I* (ed. Hornbein, T.) 473–540 (Marcel Dekker, 1981).
20. Hill, J. M. Discharge of group IV phrenic afferent fibers increases during diaphragmatic fatigue. *Brain Res.* **856**, 240–4 (2000).
21. Kaufman, M. P. & Hayes, S. G. The exercise pressor reflex. *Clin. Auton. Res.* **12**, 429–39 (2002).
22. Haverkamp, H. C., Metelits, M., Hartnett, J., Olsson, K. & Coast, J. R. Pulmonary function subsequent to expiratory muscle fatigue in healthy humans. *Int. J. Sports Med.* **22**, 498–503 (2001).
23. Orozco-Levi, M. *et al.* Expiratory muscle endurance in middle-aged healthy subjects. *Lung* **179**, 93–103 (2001).
24. Suzuki, S., Suzuki, J., Okubo, T. Expiratory muscle fatigue in normal subjects. *J. Appl. Physiol.* **70**, 2632–2639 (1991).

25. Taylor, B. J. & Romer, L. M. Effect of expiratory resistive loading on inspiratory and expiratory muscle fatigue. *Respir. Physiol. Neurobiol.* **166**, 164–74 (2009).
26. Martin, J. G. & De Troyer, A. The behaviour of the abdominal muscles during inspiratory mechanical loading. *Respir. Physiol.* **50**, 63–73 (1982).
27. Abbrecht, P. H., Rajagopal, K. R. & Kyle, R. R. Expiratory muscle recruitment during inspiratory flow-resistive loading and exercise. *Am. Rev. Respir. Dis.* **144**, 113–120 (1991).
28. Stubbing, D. G., Pengelly, L. D., Morse, J. L. & Jones, N. L. Pulmonary mechanics during exercise in normal males. *J. Appl. Physiol.* **49**, 506–10 (1980).
29. Rahn, H., Otis, A., LE, C. & Fenn, W. The pressure-volume diagram of the thorax and lung. *Am. J. Physiol.* **146**, 161–178 (1946).
30. Smith, J. & Bellemare, F. Effect of lung volume on in vivo contraction characteristics of human diaphragm. *J. Appl. Physiol.* **62**, 1893–900 (1987).
31. Henke, K. G., Sharratt, M., Pegelow, D. & Dempsey, J. A. Regulation of end-expiratory lung volume during exercise. *J. Appl. Physiol.* **64**, 135–46 (1988).
32. Grassino, A. E., Derenne, J. P., Almirall, J., Milic-Emili, J. & Whitelaw, W. Configuration of the chest wall and occlusion pressures in awake humans. *J. Appl. Physiol.* **50**, 134–42 (1981).
33. Evans, J. A. & Whitelaw, W. A. The assessment of maximal respiratory mouth pressures in adults. *Respir. Care* **54**, 1348–59 (2009).
34. Kufel, T. J., Pineda, L. a & Mador, M. J. Comparison of potentiated and unpotentiated twitches as an index of muscle fatigue. *Muscle Nerve* **25**, 438–44 (2002).
35. Kufel, T. J., Pineda, L. A., Junega, R. G., Hathwar, R. & Mador, M. J. Diaphragmatic function after intense exercise in congestive heart failure patients. *Eur. Respir. J.* **20**, 1399–1405 (2002).
36. Enoka, R. M. & Duchateau, J. Muscle fatigue: what, why and how it influences muscle function. *J. Physiol.* **586**, 11–23 (2008).

37. Reid, W. D. & Dechman, G. Considerations when testing and training the respiratory muscles. *Phys. Ther.* **75**, 971–82 (1995).
38. Abe, T., Kusuhara, N., Yoshimura, N., Tomita, T. & Easton, P. A. Differential respiratory activity of four abdominal muscles in humans. *J. Appl. Physiol.* **80**, 1379–89 (1996).
39. Witt, J. D., Guenette, J. A., Rupert, J. L., McKenzie, D. C. & Sheel, A. W. Inspiratory muscle training attenuates the human respiratory muscle metaboreflex. *J. Physiol.* **584**, 1019–28 (2007).
40. Bonde-Petersen, F., Mork, A. L. & Nielsen, E. Local muscle blood flow and sustained contractions of human arm and back muscles. *Eur. J. Appl. Physiol. Occup. Physiol.* **34**, 43–50 (1975).
41. Bellemare, F. & Grassino, A. Effect of pressure and timing of contraction on human diaphragm fatigue. *J. Appl. Physiol.* **53**, 1190–5 (1982).
42. Bellemare, F., Wight, D., Lavigne, C. M. & Grassino, A. Effect of tension and timing of contraction on the blood flow of the diaphragm. *J. Appl. Physiol.* **54**, 1597–606 (1983).
43. Bigland-Ritchie, B. Muscle fatigue and the influence of changing neural drive. *Clin. Chest Med.* **5**, 21–34 (1984).
44. Fitts, R. H. Cellular, molecular, and metabolic basis of muscle fatigue. In *Handbook of Physiology, Exercise: Regulation and Integration of Multiple Systems* (eds. Rowell, L. B. & Shepherd, J. T.) 1151–1183 (American Physiological Society, 1996).
45. Westerblad, H., Duty, S. & Allen, D. G. Intracellular calcium concentration during low-frequency fatigue in isolated single fibers of mouse skeletal muscle. *J. Appl. Physiol.* **75**, 382–8 (1993).
46. Jammes, Y. & Speck, D. Respiratory control by respiratory and diaphragmatic muscle afferents. In *Regulation of Breathing* (eds. Dempsey, J. A. & Pack, A. I.) 543–582 (Marcel Dekker, 1995).
47. Dempsey, J. A., Sheel, A. W., St. Croix, C. M. & Morgan, B. J. Respiratory influences on sympathetic vasomotor outflow in humans. *Respir. Physiol. Neurobiol.* **130**, 3–20 (2002).

48. McKenzie, D. K., Allen, G. M., Butler, J. E. & Gandevia, S. C. Task failure with lack of diaphragm fatigue during inspiratory resistive loading in human subjects. *J. Appl. Physiol.* **82**, 2011–2019 (1997).
49. Gorman, R. B., McKenzie, D. K. & Gandevia, S. C. Task failure, breathing discomfort and CO₂ accumulation without fatigue during inspiratory resistive loading in humans. *Respir. Physiol.* **115**, 273–86 (1999).
50. Rohrbach, M., Perret, C., Kayser, B., Boutellier, U. & Spengler, C. M. Task failure from inspiratory resistive loaded breathing: a role for inspiratory muscle fatigue? *Eur. J. Appl. Physiol.* **90**, 405–410 (2003).
51. Wragg, S. *et al.* Potentiation of diaphragmatic twitch after voluntary contraction in normal subjects. *Thorax* **49**, 1234–7 (1994).
52. Guenette, J. a *et al.* Sex differences in exercise-induced diaphragmatic fatigue in endurance-trained athletes. *J. Appl. Physiol.* **109**, 35–46 (2010).

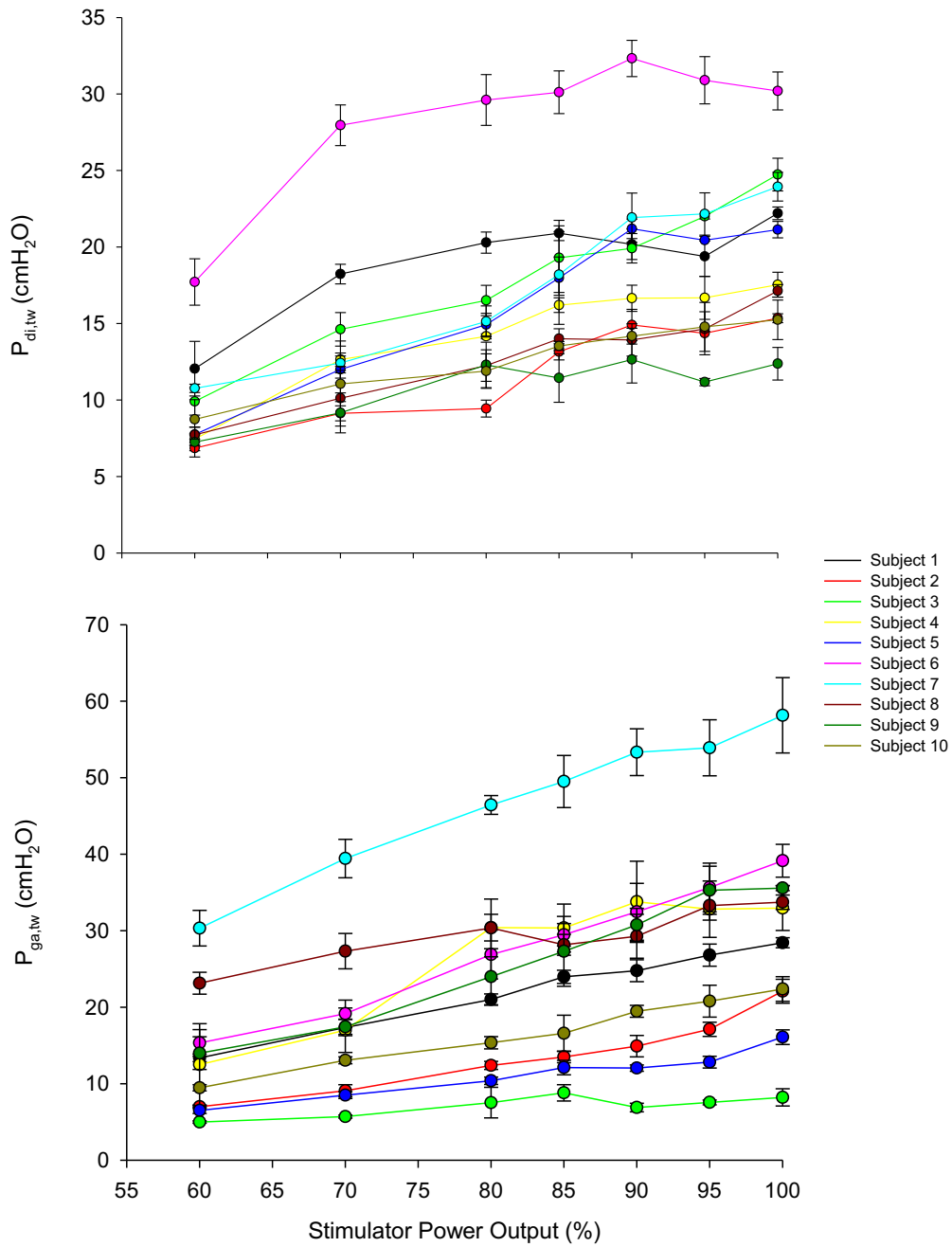
Appendix A: Individual subject data

Table 14: Individual descriptive data for all subjects.

Subject	1	2	3	4	5	6	7	8	9	10
Height	167	175	180	186	184	174	181	181	185	196
Weight	64	75	65	70	87	79	72	74	73	100
Age	23	27	20	28	24	26	28	25	28	23
FVC	5.78	4.13	4.98	5.37	6.08	4.29	5.63	6.08	5.99	7.16
FVC % predicted	124	82	89	95	108	86	105	112	107	113
FEV1	4.58	3.55	4.65	4.85	5.04	3.34	4.69	4.98	4.81	5.85
FEV1% predicted	114	84	100	103	107	78	105	109	103	111
FEV1/FVC	79.2	86	95.3	90.3	82.9	77.9	83.3	81.9	80.3	81.7
FEV1/FVC% predicted	95	104	114	110	100	94	101	99	98	98
PEF	11.4	9.68	10.4	12.1	9.65	10.2	13.3	11.0	12.1	9.43
PEF% predicted	121	99	101	117	93	105	133	108	117	84
MIP	120	103.8	161	75	105.2	124.6	125.8	106.4	117.2	116.5
MEP	98.6	78.2	146	115.4	146.2	178.1	107.5	116.5	153.0	123.25
P _{diMAX}	101.9	109.8	116.2	113.0	105.3	106.25	95.15	156.8	136.1	146.2
P _{gaMAX}	144.5	137.1	170.6	154.25	155.8	164	134.5	165.42	167	113

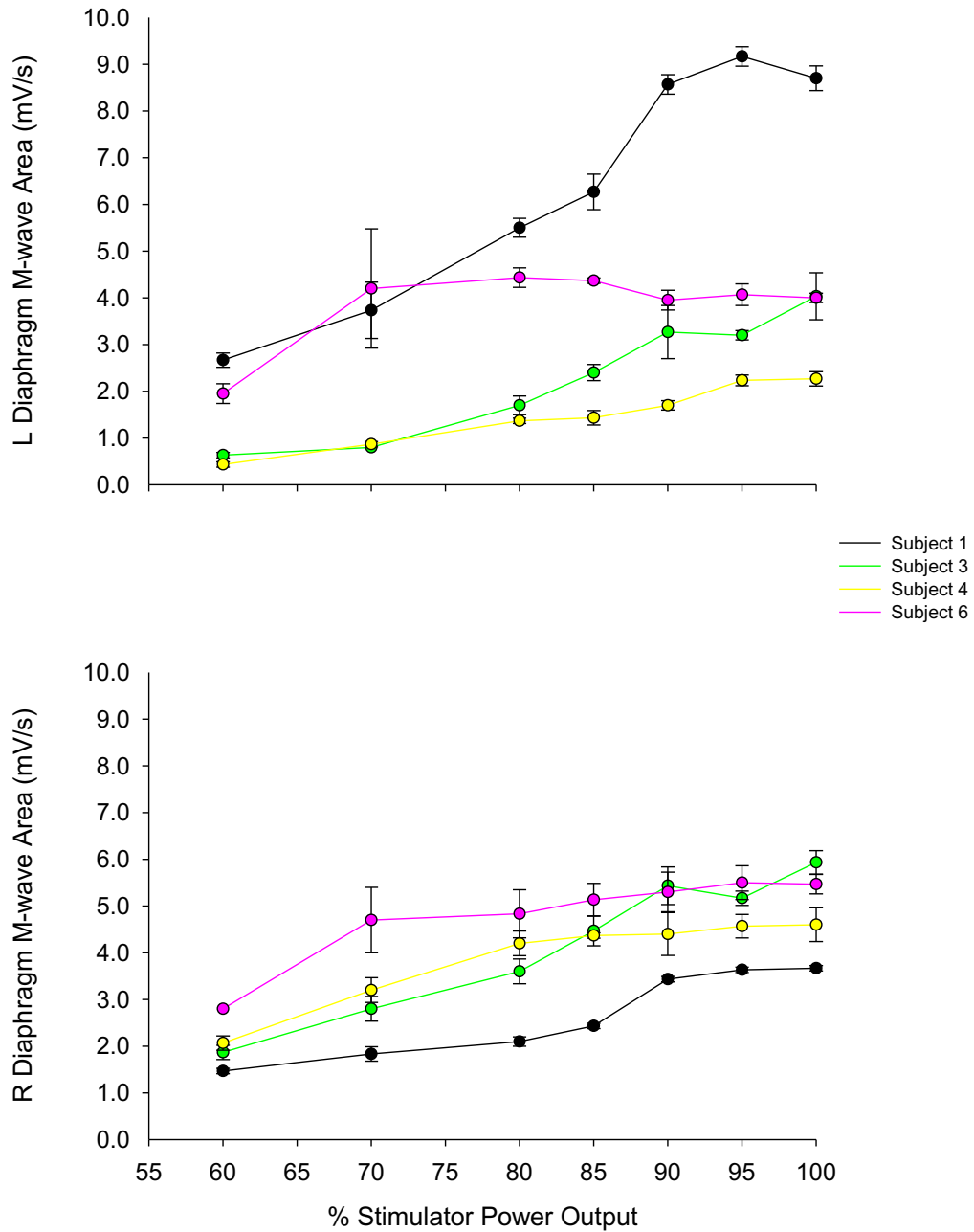
Legend: FVC, forced vital capacity; FEV₁, forced expiratory volume in 1 s; PEF, peak expiratory flow; MIP, maximal inspiratory pressure; MEP, maximal expiratory pressure; P_{diMAX}, maximal transdiaphragmatic pressure; P_{gaMAX}, maximal gastric pressure.

Figure 16: Individual transdiaphragmatic and gastric twitch pressures in response to 1-Hz magnetic stimulation of increasing stimulation intensity



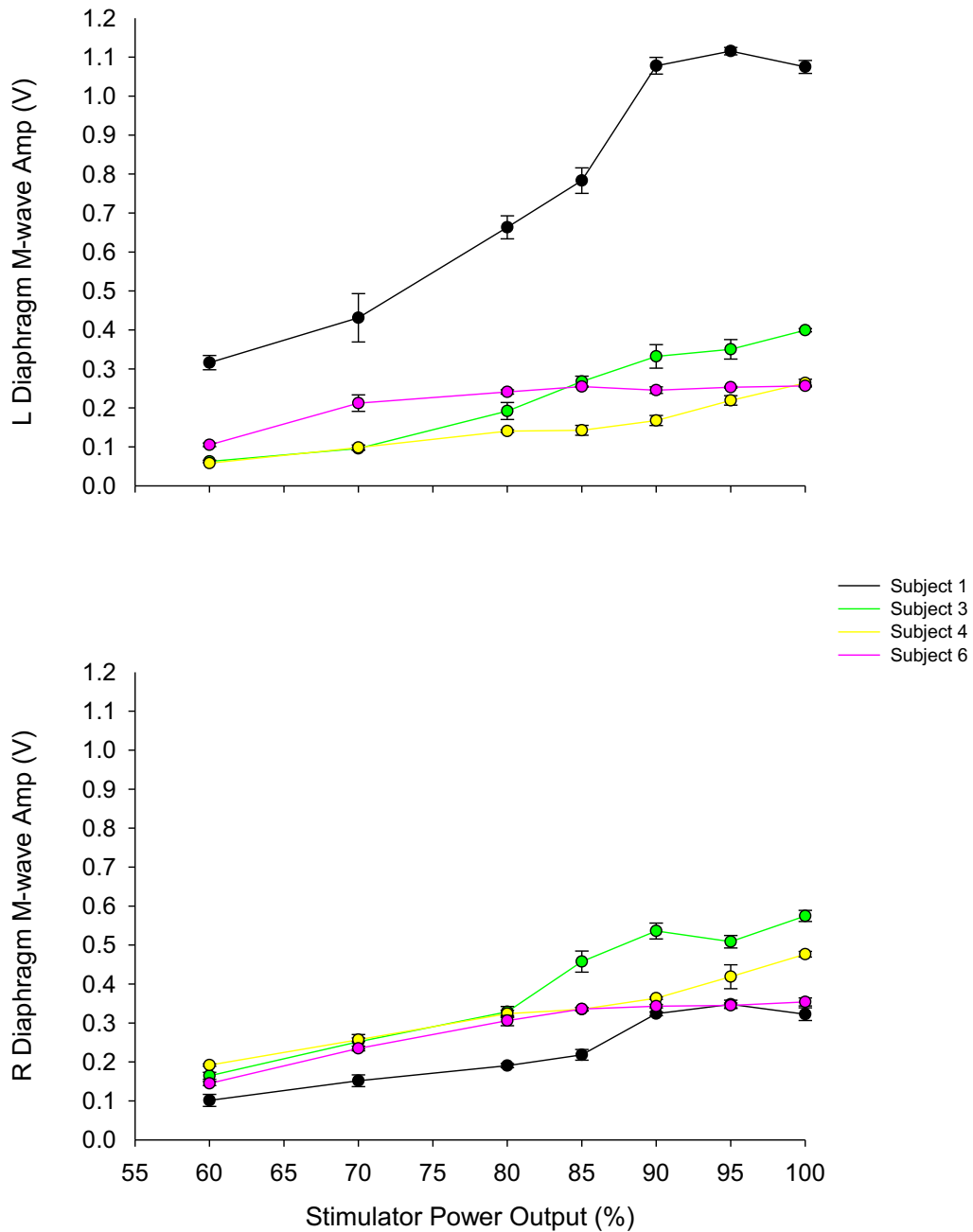
Legend: Values are means \pm SD. $P_{di,tw}$, transdiaphragmatic twitch pressure; $P_{ga,tw}$, gastric twitch pressure.

Figure 17: Individual left and right diaphragm M-wave areas in response to 1-Hz magnetic stimulation of increasing stimulation intensity



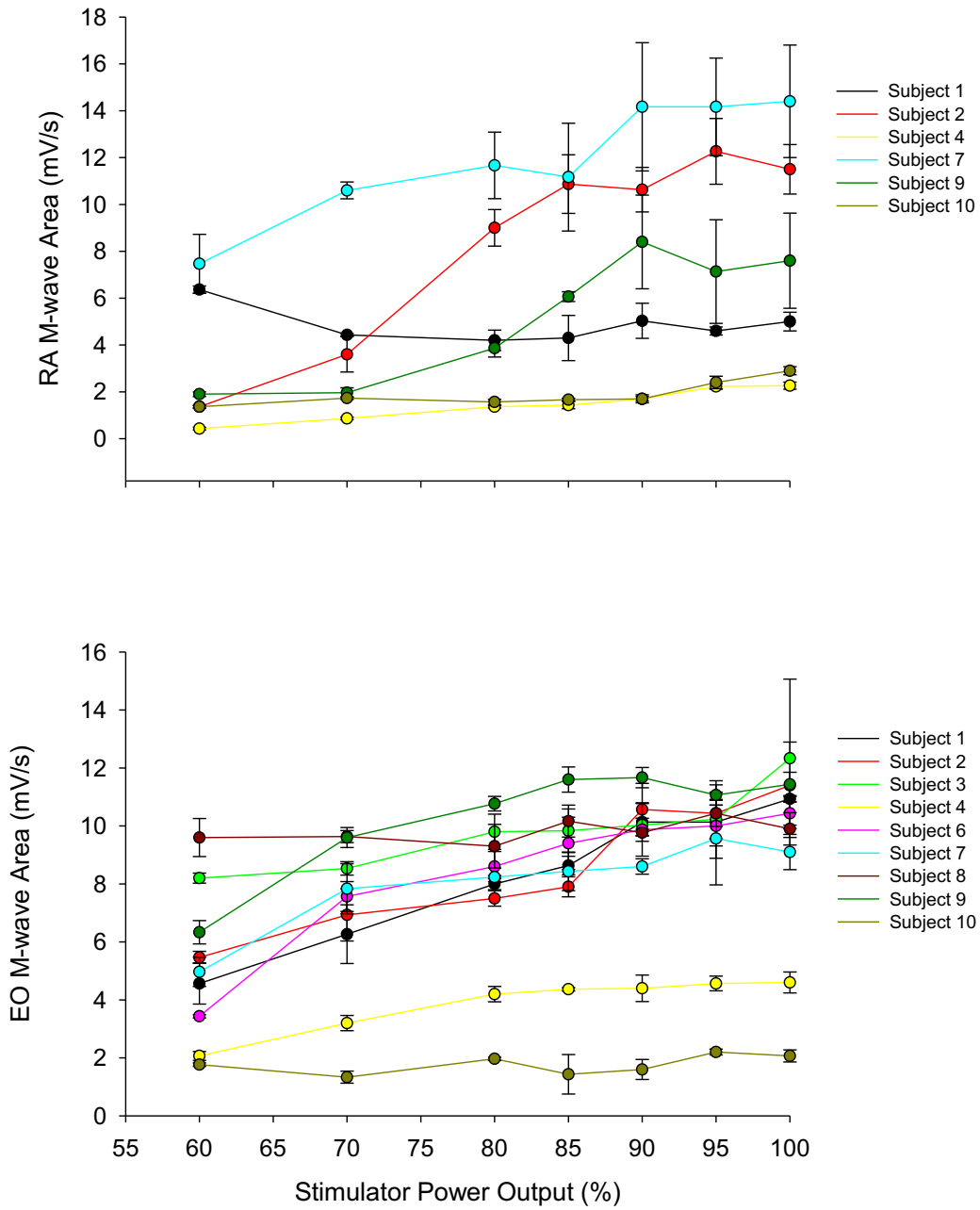
Legend: Values are means \pm SD.

Figure 18: Individual left and right diaphragm M-wave amplitudes in response to 1-Hz magnetic stimulation of increasing stimulation intensity



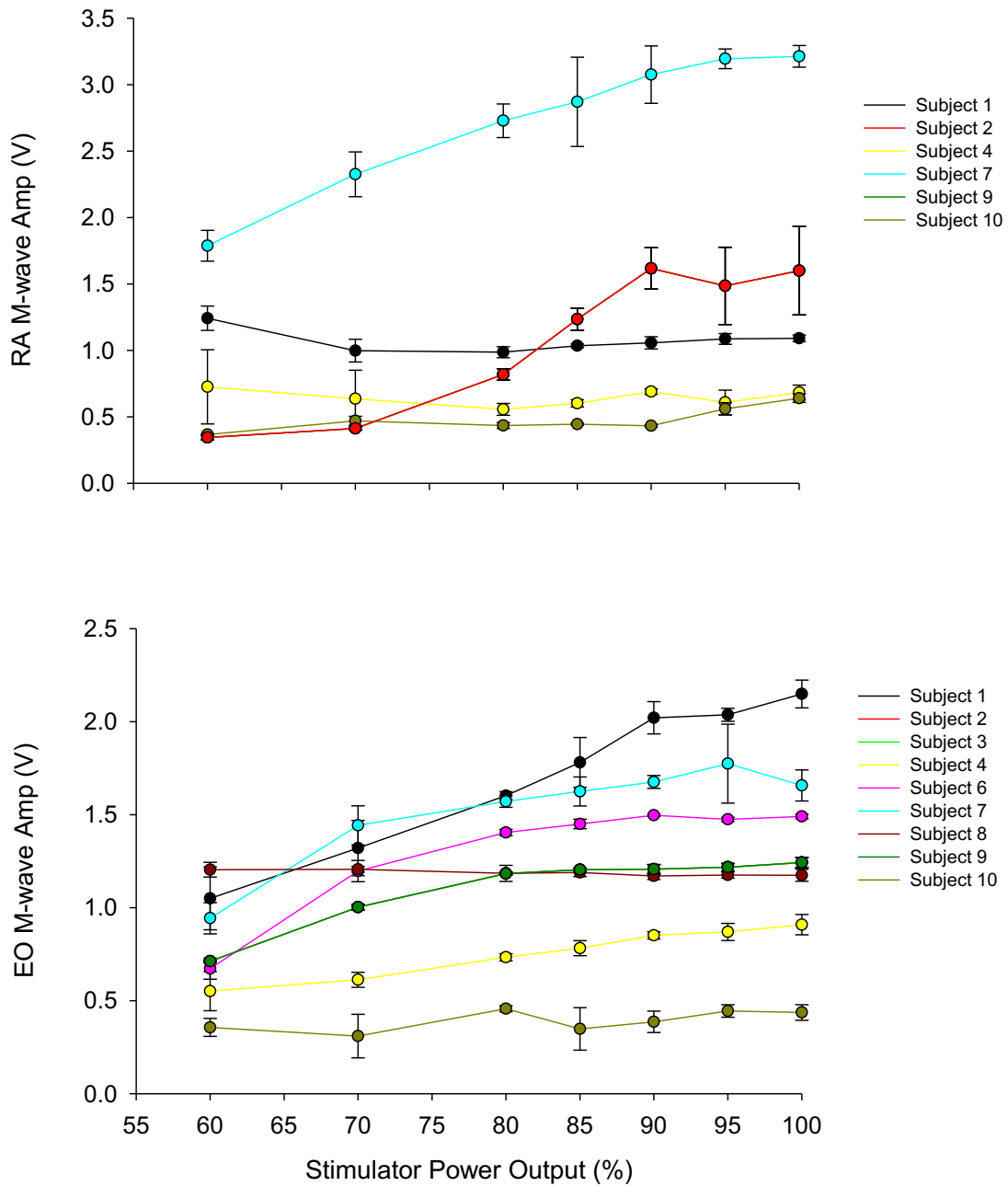
Legend: Values are means \pm SD.

Figure 19: Individual rectus abdominis and external oblique M-wave areas in response to 1-Hz magnetic stimulation of increasing stimulation intensity



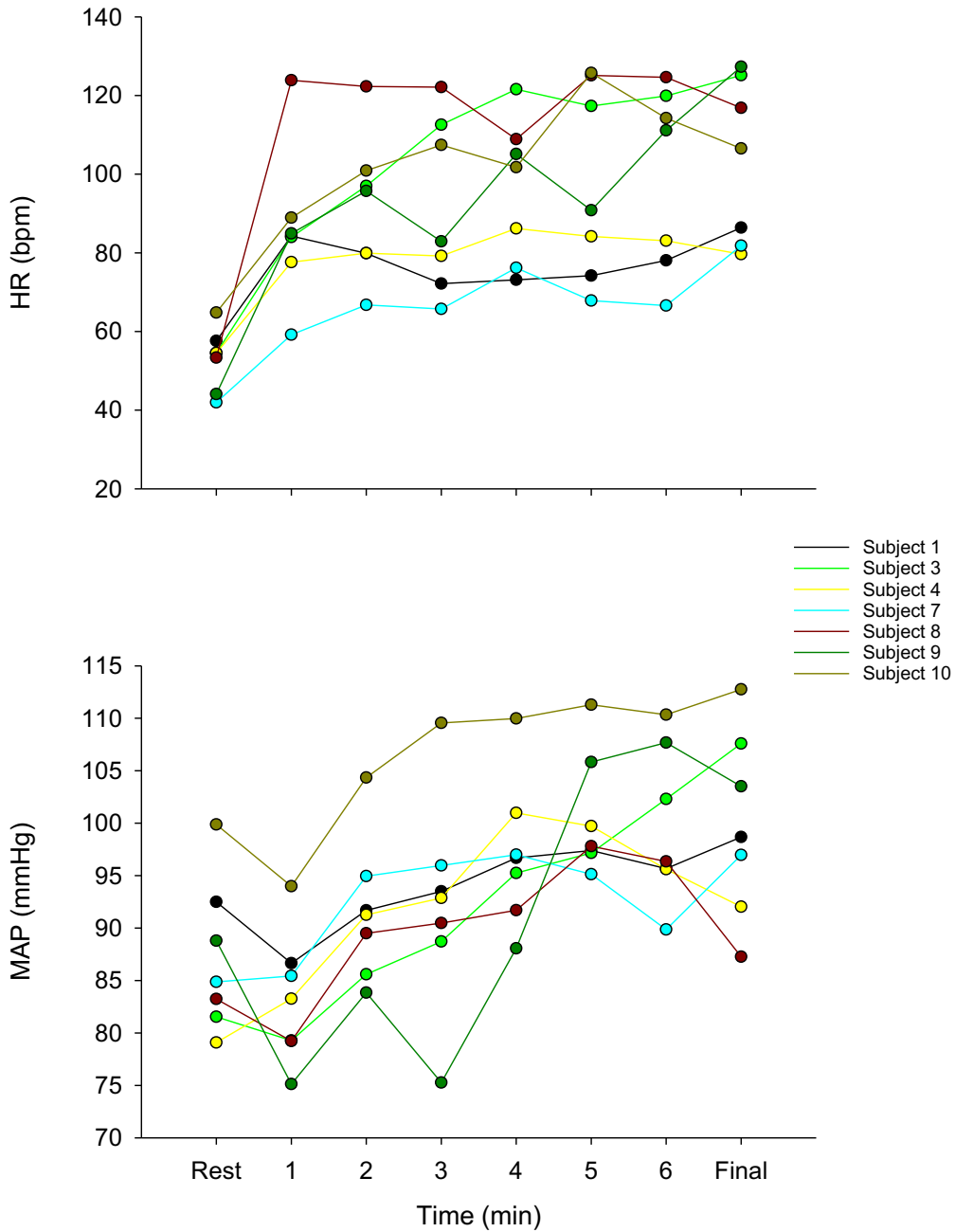
Legend: Values are means \pm SD. RA, rectus abdominis; EO, external oblique. Note that RA graph shows data from 6 subjects, while EO graph shows data from 9 subjects.

Figure 20: Individual rectus abdominis and external oblique M-wave amplitudes in response to 1-Hz magnetic stimulation of increasing stimulation intensity



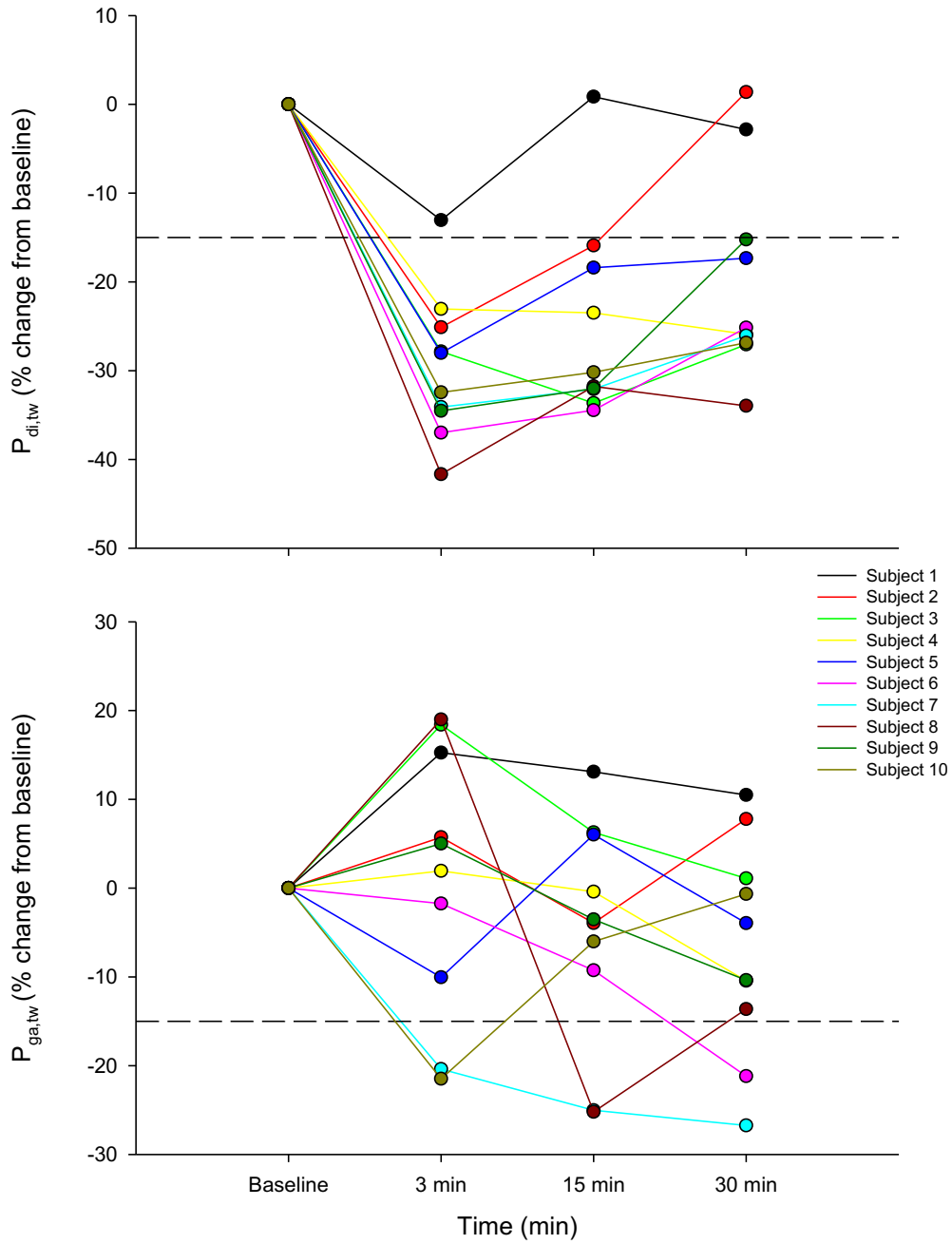
Legend: Values are means \pm SD. RA, rectus abdominis; EO, external oblique. Note that RA graph shows data from 6 subjects, while EO graph shows data from 9 subjects.

Figure 21: Individual heart rate and blood pressure data at rest, during the first 6 min, and during the final min of inspiratory loading.



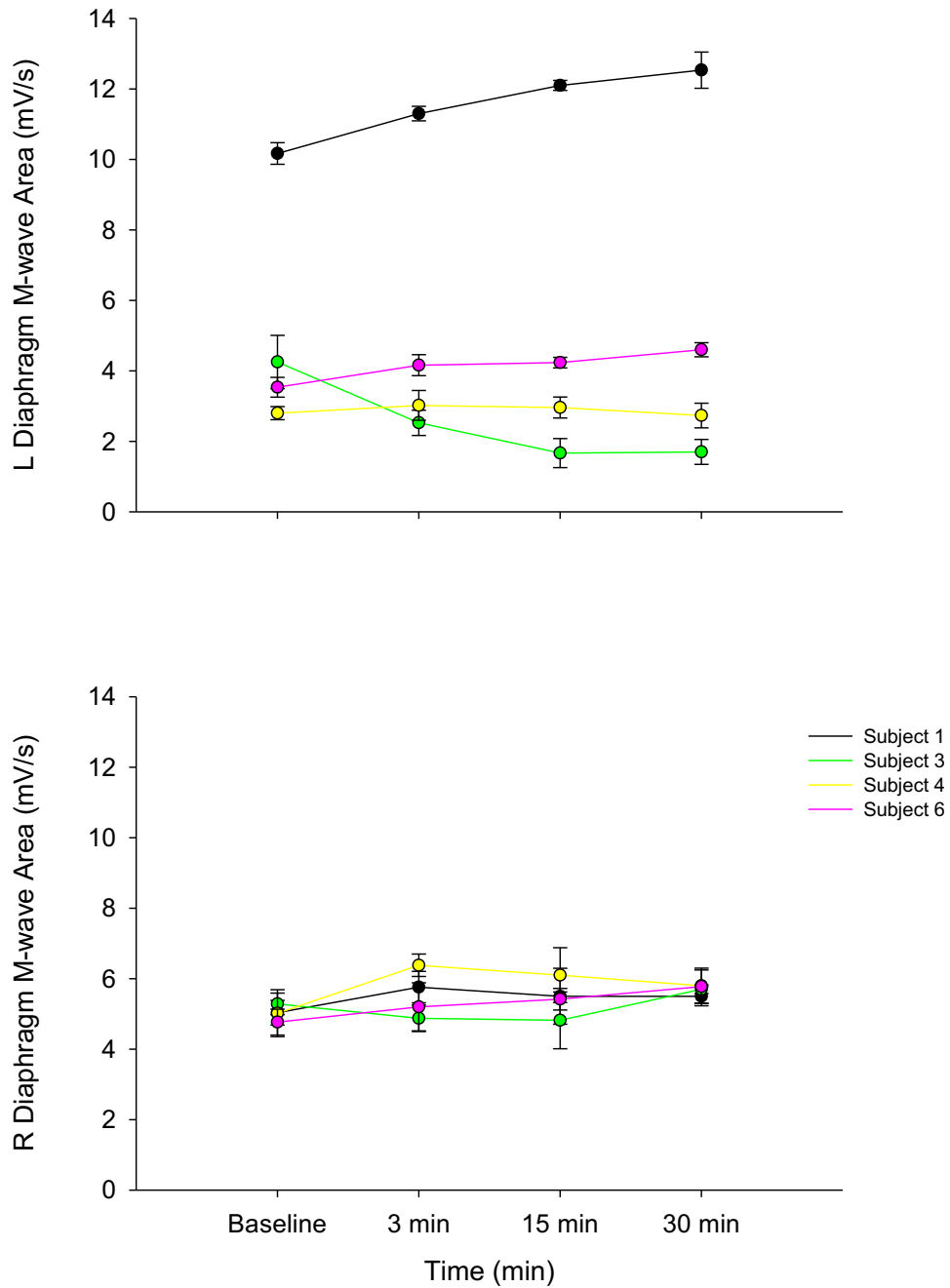
Legend: Values are means for each subject at each time point. HR, heart rate; MAP, mean arterial pressure.

Figure 22: Individual transdiaphragmatic and gastric pressure percent changes from baseline at 3 min-, 15 min-, and 30 min-post IRL.



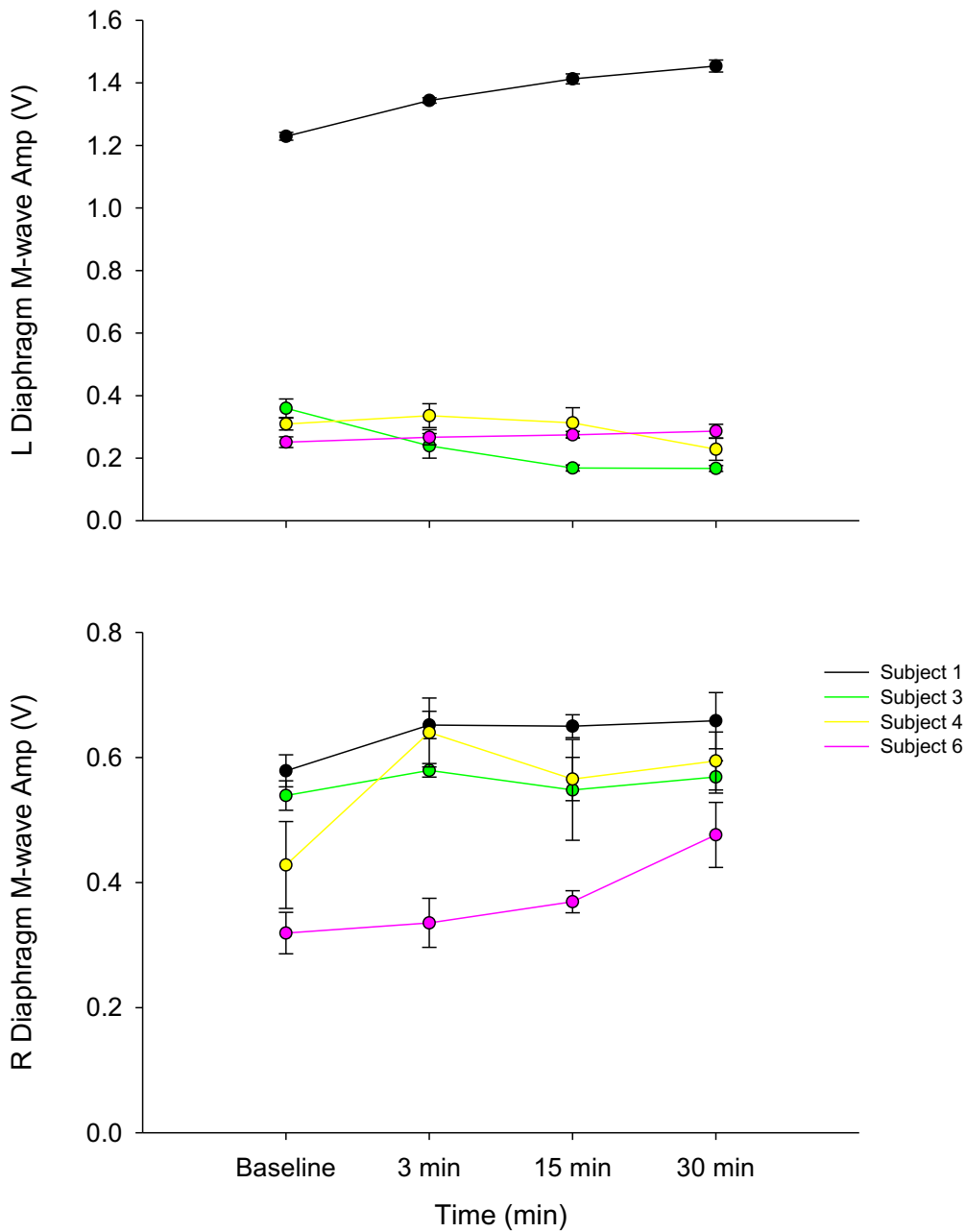
Legend: Values are means for each subject at each time point. Zero represents baseline. The dashed line represents the 15% reduction in twitch pressure used as the threshold of fatigue.

Figure 23: Individual left and right diaphragm M-wave area in response to 1-Hz magnetic stimulation at baseline, 3 min post-, 15 min post-, and 30 min post-IRL.



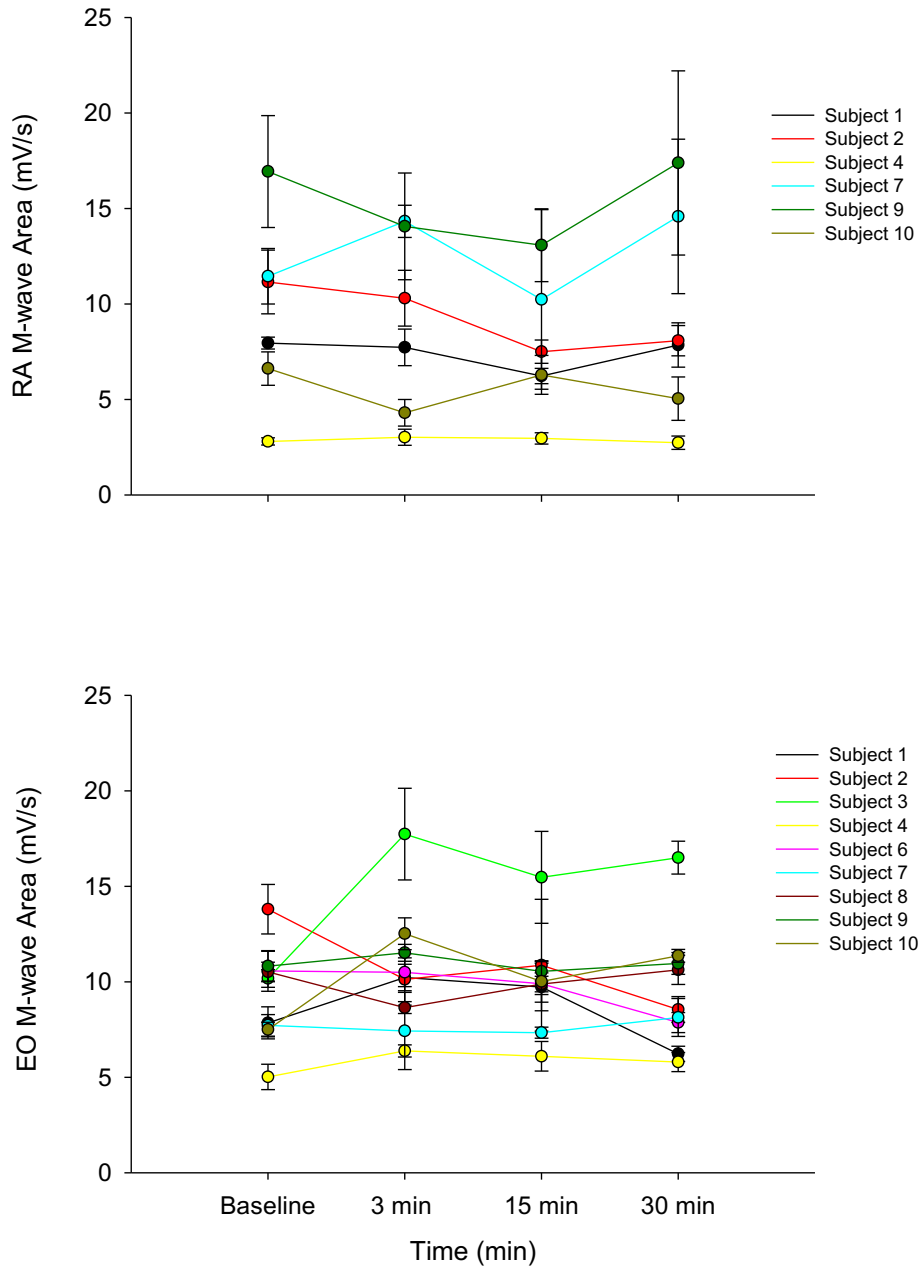
Legend: Values are means \pm SD.

Figure 24: Individual left and right diaphragm M-wave amplitude in response to 1-Hz magnetic stimulation at baseline, 3 min post-, 15 min post-, and 30 min post-IRL.



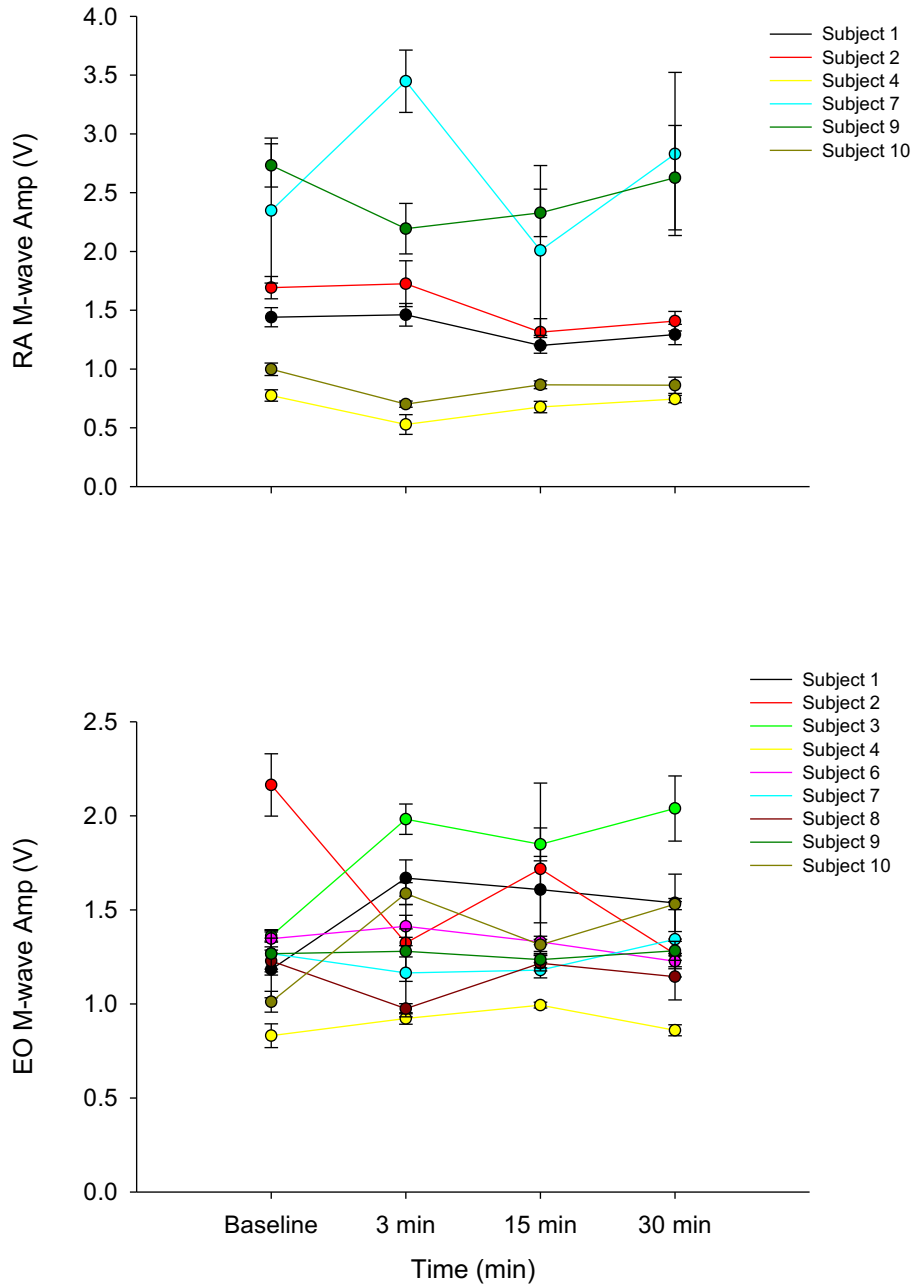
Legend: Values are means \pm SD.

Figure 25: Individual rectus abdominis and external oblique M-wave area in response to 1-Hz magnetic stimulation at baseline, 3 min post-, 15 min post-, and 30 min post-IRL.



Legend: Values are means \pm SD. RA, rectus abdominis; EO, external oblique. Note that RA graph shows data from 6 subjects, while EO graph shows data from 9 subjects.

Figure 26: Individual rectus abdominis and external oblique M-wave amplitude in response to 1-Hz magnetic stimulation at baseline, 3 min post-, 15 min post-, and 30 min post-IRL.



Legend: Values are means \pm SD. RA, rectus abdominis; EO, external oblique. Note that RA graph shows data from 6 subjects, while EO graph shows data from 9 subjects.